National Aeronautics and Space Administration

In Search of Ocean Worlds in the Uranian System & Kuiper Belt

PLANETARY MISSION CONCEPT STUDY FOR THE 2023–2032 DECADAL SURVEY

14 May 2021

Calypso

Emily S. Martin
Science Co-Lead
National Air and Space Museum,
Smithsonian Institution
martines@si.edu

William F. Bottke
Science Co-Lead
Southwest Research Institute
bottke@boulder/swri.edu

Chris B. Hersman
Study Lead
Johns Hopkins University
Applied Physics Laboratory
chris.hersman@jhuapl.edu

www.nasa.gov

Data Release, Distribution & Cost Interpretation Statements

This document is intended to support the 2023–2032 Planetary Science and Astrobiology Decadal Survey.

The data contained in this document may not be modified in any way.

Cost estimates described or summarized in this document were generated as part of a preliminary concept study, are model-based, assume an APL in-house build, and do not constitute a commitment on the part of APL.

Cost reserves for development and operations were included as prescribed by the NASA ground rules for the Planetary Mission Concept Studies program. Unadjusted estimate totals and cost reserve allocations would be revised as needed in future more-detailed studies as appropriate for the specific cost-risks for a given mission concept.

Acknowledgements

The Johns Hopkins Applied Physics Laboratory would like to thank all of the Calypso team members, the National Academies of Sciences, Engineering, and Medicine Planetary Science and Astrobiology Decadal Survey 2023–2032 (especially the Small Bodies Panel and the Ocean Worlds and Dwarf Planets Panel), and the NASA Planetary Science Division for supporting this study.

ROLE	NAME	AFFILIATION
Science Team		
Leadership	Emily Martin, Science Co-Lead	Smithsonian/NASM
	William Bottke, Science Co-Lead	SwRI
	Glen Fountain, Management	APL
Science	Julie Castillo-Rogez	JPL
	Nancy Chabot	APL
	Ian Cohen	APL
	Alex Hayes	Cornell
	Marc Neveu	NASA/GSFC
	Lynnae Quick	NASA/GSFC
	Carol Raymond	JPL
	Kirby Runyon	APL
	Audrey Thirouin	Lowell
	Benjamin Weiss	MIT
Engineering Team		
Study Design Lead/MSE	Chris Hersman	APL
Project Management	Dewey Adams	APL
RF/Communications	Reza Ashtari	APL
Harness Design	Vince Bailey	APL
Scheduling	Dewey Barlow	APL
Operations	Alice Bowman	APL
Propulsion	Stewart Bushman	APL
Avionics	Christian Campo	APL
Avionics	Steve Cho	APL
Radiation Design & Mitigation	Michelle Donegan	APL
Thermal Engineering	Jack Ercol	APL
Scheduling	Norm Evans	APL
Ground Support	Mike Furrow	APL
Flight Software	Brandon Haber	APL
MSE Support	Max Harrow	APL
Power Design	Chris Hersman	APL
Flight Software	Adrian Hill	APL
MSE Support	Marc Hoffman	APL
Guidance Navigation & Control	Jack Hunt	APL
Avionics	Justin Kelman	APL
Mechanical/Structure	Felipe Ruiz	APL
Mission Design & Analysis	Wayne Schlei	APL
Cost Modeling	Rachel Sholder	APL
Mission Design & Analysis	Fazle Siddique	APL
Payload	Kim Slack	APL
Avionics	Kirk Volland	APL
Designer	David Weir	APL
Integration & Test	Jay White	APL
Report Development Team		
Editing	Marcie Steerman	APL

In Search of Ocean Worlds in the Uranian System & Kuiper Belt

PLANETARY MISSION CONCEPT STUDY FOR THE 2023–2032 DECADAL SURVEY

How Diverse Are Ocean Worlds?

Water is the most fundamental element of habitability, and finding water beyond Earth has long been the focus of our search for life. NASA's *Roadmap for Ocean Worlds* outlined several potential missions to bodies where we might find water ... and, potentially, life. The highest priority, like Europa Clipper and Dragonfly, are already in advanced planning. Other destinations, like Enceladus and Triton, are attractive because of what we already know about them. However, the Uranian moons and Kuiper Belt objects were prioritized for habitability exploration because of what we have yet to learn about them.

The Calypso mission would target and explore the mysteries of ocean worlds far more distant than those visited by the famed Jacques Cousteau vessel for which it's named. Specifically, Calypso would focus on *finding the limits on and pathways to ocean world formation and evolution in two very different contexts: ice giant systems and planetesimals formed beyond the giant planets.*

Calypso Goals

Uranian Moon (Ariel Baselined)

- Search for subsurface ocean and nature of internal structure
- Explore geologic history and surface composition
- Characterize crater populations
- Study Uranus, rings, ring moons, and satellites

KBO/Dwarf Planet (G!kún‖'hòmdímà Baselined**)**

- Characterize global geology and morphology, including rotational and physical properties
- Map surface composition and volatile distribution
- Characterize crater populations
- Search for satellites and rings

Understanding Ocean World Evolution

Scientists find it plausible that the five largest moons around Uranus and dwarf planets in the Kuiper Belt had or currently have subsurface oceans. The opportunity to better understand and characterize these "ocean worlds" and their hydrospheres make them ideal candidates for the continued scientific exploration and search for habitable environments within our solar system.

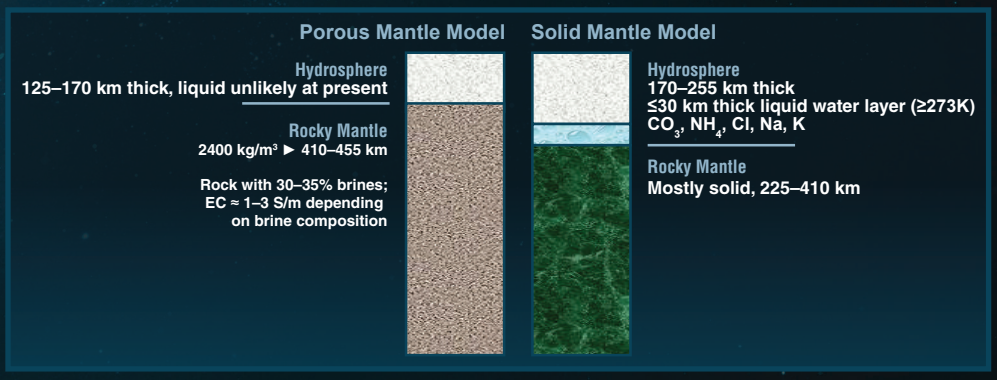

Calypso will test competing interior models of Ariel through electromagnetic induction, with a subsurface ocean producing a secondary magnetic field potentially detectable by a magnetometer (after Neveu [2019] (left) and Castillo-Rogez et al. [2019] (right)).

Calypso

Calypso
DESIGN STUDY

Mission Design Provides Numerous Launch Opportunities

Calypso includes traveling through the Uranian system with a flyby of a Uranian moon (Ariel or Miranda), then a close encounter with one of several possible KBOs that are plausible ocean worlds. Ariel and G!kúnll'hòmdímà are baselined, but Calypso science is flexible – enabling target flexibility in keeping with uncertainties of future New Frontiers announcements and mission launch windows. Numerous annual launch scenarios are possible (below), including several that do not require a Jupiter encounter (see report).

Launch Year	Launch Date	Jupiter Encounter	Ocean World Encounter	Dwarf Planet Encounter	Ocean World	Dwarf Planet	C3 (km^2/s^2)	Time of Flight (years)
2035	Jul 2035	Nov 2036	Nov 2041	Sep 2052	Ariel	G!kúnll'hòmdímà	121	17.1
2034	Jul 2034	Feb 2036	Oct 2041	Sep 2053	Ariel	G!kúnll'hòmdímà	120	19.2
2034	Jul 2034	Jan 2036	Feb 2041	Aug 2051	Miranda	Chaos	120	17.1
2034	Jul 2034	Mar 2036	Jul 2042	Jul 2055	Ariel	Varuna	135	21.0
2034	Jul 2034	Feb 2036	Aug 2041	Jan 2052	Miranda	Varuna	135	17.5
2035	Jul 2035	Nov 2036	May 2041	May 2051	Miranda	Chaos	120	15.8
2035	Aug 2035	Dec 2036	Feb 2042	Jan 2053	Miranda	Varuna	135	17.4
2035	Aug 2035	Dec 2036	Jan 2043	Nov 2056	Ariel	Varuna	135	21.3
2036	Sep 2036	Sep 2037	Apr 2042	Nov 2053	Ariel	Chaos	162	17.2
2036	Sep 2036	Oct 2037	Feb 2043	Apr 2055	Miranda	Varuna	150	18.6

Calypso Baseline

Spacecraft & Instrument Suite Draw on Substantial Heritage

Narrow Angle Camera (NAC): New Horizons LORRI

Vis/NIR Imaging Spectrometer (Vis/NIR): New Horizons RALPH

Radio Science (RS): New Horizons REX

Ultraviolet Imaging Spectrometer[1] (UVIS): New Horizons ALICE

Dust Counter[1] (D-Count): New Horizons SDC

Magnetometer (Mag): MESSENGER MAG

Ion Electrostatic Analyzer[1,2] (I-ESA): IMAP SWAPI

Electron Electrostatic Analyzer[1,2] (E-ESA): Parker Solar Probe SPAN-B

Energetic Particle Detector[1] (EPD): MMS EIS

1. Potential Descope
2. Either I-ESA or E-ESA may be descoped, but not both

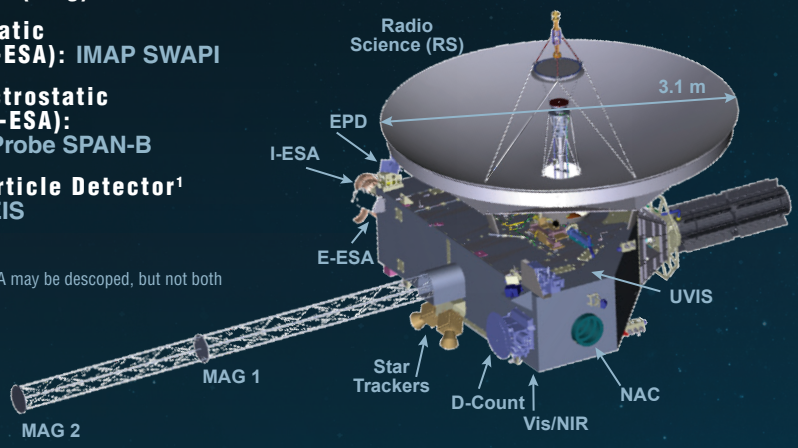

Proven New Horizons Design: Enhanced Structure for 3.1-m Antenna; Added Magnetometer Boom; Reoriented Optical Instruments

Energy Efficient: 18-Year Mission with Single RTG

Flexible Communications: Dual X-Band/Ka-Band Communications

Launch Vehicle Needs Less Demanding than New Horizons: MPV Wet Mass 835 kg; Max C3: 121 km^2/s^2

Stowed Dimensions: 363 x 338 x 272 cm

Launch Configurations: STAR 48BV + Vulcan or Falcon Heavy Expendable

Mission Costs Comparable to Other New Frontiers Missions

	FY$25K w/o LV	FY$25K w/ LV
A–D Subtotal	567,037	843,037
A–D Reserves	283,519	283,519
RTG Surcharge	26,000	26,000
A–D PIMMC	876,556	1,152,556
E–F Subtotal	533,133	533,133
E–F Reserves	126,084	126,084
E–F PIMMC	659,217	659,217
Total PIMMC	1,535,773	1,811,773

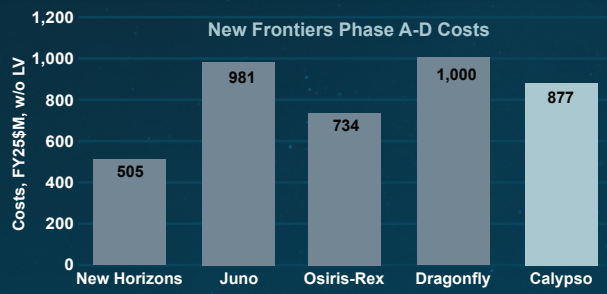

Planetary Science Decadal Survey

Calypso Mission Concept Design Study Final Report

Executive Summary

Discovering liquid water, one of the foundational building blocks for sustaining life, has long been a focus of the search for life beyond our own planet. While Earth remains the only known body in our solar system with liquid water at its surface, there are other worlds that have shown direct evidence of, or characteristics associated with, the presence of subsurface oceans concealed under ice shells. Scientists find it plausible that the five largest moons around Uranus, as well as dwarf planets in the Kuiper Belt, likely had or currently have subsurface oceans. The opportunity to better understand and characterize these "ocean worlds" and their hydrospheres make them ideal candidates for the continued scientific exploration and search for habitable environments within our solar system.

The Calypso mission seeks to determine the pathways to and limits on ocean world formation. To this end, the Calypso planetary mission concept study (PMCS) provides a point design for a New Frontiers-class mission to a Uranian satellite and a dwarf planet in the Kuiper Belt in search of new scientific evidence of the existence of subsurface oceans. Our highest priority science centers on the study of the internal structures and surface characteristics for each of the two candidate bodies proposed for the baseline science mission. Calypso also presents an opportunity to learn more about these worlds as well as the systems where they reside. This study report represents a concept maturity level of 4 (CML-4), including details of the proposed spacecraft's estimated subsystem-level mass, power and expected performance. The spacecraft design and mission architecture, along with its associated risk and cost analyses, demonstrate the viability of the Calypso mission concept within the parameters of a New Frontiers mission and the PMCS study guidelines, provided that a high performance launch vehicle can be used for this mission.

Calypso's baseline mission is a flyby of Ariel, the fourth-largest moon orbiting Uranus, and the subsequent flyby of (229762) G!kún‖'hòmdímà, a Kuiper belt dwarf planet with a sizable moon called G!ò'é !Hú. Launching in 2035 on a Falcon 9 Heavy Expendable launch vehicle with a STAR48VB kick stage, the Calypso spacecraft will make use of a gravity-assisted flyby of Jupiter a year into its cruise phase before arriving at the Uranian system in 2041. The spacecraft will then continue on towards the Kuiper Belt with an encounter of G!kún‖'hòmdímà in 2052. The baseline design includes sufficient spacecraft resources to facilitate a flyby of an additional Kuiper Belt object (KBO) beyond G!kún‖'hòmdímà, should a suitable candidate be identified for an extended mission, and statistical analysis indicates at least one larger than 20 km is expected.

This is only one of several different viable mission options. Annual launch dates between 2028–2042 make it possible to visit a Uranian moon like, Miranda or Ariel, plus one of several KBO dwarf planet(s) within ~20 years of launch, and none of them require a Jupiter gravity assist. This flexibility allows Calypso to readily deal with any vagaries in the timing of New Frontiers' announcements of opportunities.

The conceptual design of Calypso is based on the proven design of the New Horizons spacecraft which successfully completed similar flyby encounters of Pluto in 2015 and, subsequently, the KBO Arrokoth in 2019. Like New Horizons, Calypso will use a single radioisotope thermoelectric generator (RTG) as its sole source of power. High-resolution cameras will collect imagery of Uranus, Ariel, and other moons and rings in the Uranian system during a near encounter before obtaining <300-meter resolution panchromatic and color imagery of Ariel's surface to support geological and geomorphic studies. Two magnetometers attached to a deployed boom will measure Ariel's induced magnetic field in search of evidence of a subsurface ocean, while uplink radio science and plasma and dust instruments will take data simultaneously to characterize the Uranian environment. Similar sequences of observations will be taken during the flyby of G!kún‖'hòmdímà, though here geologic, compositional, and gravity evidence will provide the primary means of deducing a subsurface ocean. Outside of each encounter, Calypso's payload will measure the plasma, particle, and dust environments during the spacecraft's journey through the solar system.

The Phase A–D mission cost estimate (with 50% unencumbered reserves, excluding the launch vehicle) is $877M (FY25$), comparing favorably with past New Frontiers missions, as well as to the cost cap prescribed in the New Frontiers 4 AO (~$1.1B FY25$). This cost estimate demonstrates that the Calypso mission is feasible and compelling as a New Frontiers-class mission in the coming decade.

1. Scientific Objectives

1.1 Science Motivation

Discovering liquid water, one of the foundational building blocks for sustaining life, has long been a focus of the search for life beyond our own planet. While Earth remains the only known body in our solar system with liquid water at its surface, there are other worlds that have shown direct evidence of, or characteristics associated with, the presence of subsurface oceans concealed under ice shells. The opportunity to better understand and characterize these "ocean worlds" and their hydrospheres make them ideal candidates for the continued scientific exploration and search for habitable environments within our solar system.

The Calypso mission endeavors to explore the mysteries of ocean worlds far more distant than those visited by the famed Jacques Cousteau vessel for which it's named. Our mission design concept is twofold. First, we focus on our science goal, namely, ***finding the limits on and pathways to ocean world formation and evolution in two very different contexts: ice giant systems and planetesimals formed beyond the giant planets.*** Second, we maintain target flexibility in keeping with the uncertainties of future New Frontiers announcements and mission launch windows.

NASA's *Roadmap for Ocean Worlds* (ROW) [Hendrix et al. 2019] outlined a number of high-priority destinations in the search for ocean worlds. Missions, like Europa Clipper and Dragonfly to Titan, are already in the advanced planning stages supporting the highest priority destinations. Destinations, like Enceladus and Triton, are attractive because of what we already know about them. ROW also prioritized ice giant satellites and Kuiper Belt objects (KBOs) as the next most important targets for exploring habitability because of what we have yet to learn about them.

While the Calypso mission is highly flexible (see §3.3 for options), the baseline includes traveling through the Uranian system with a flyby of Miranda or Ariel and then a flyby of one of several dwarf planet KBOs that are plausible ocean worlds according to existing theories and observations of outer main belt asteroids [e.g., Raymond et al. 2020; Vernazza et al. 2020; Carry et al. 2021]. The close passage near Miranda or Ariel will offer an opportunity to measure its magnetic induction signal for evidence of a subsurface ocean [e.g., Weiss et al. 2020, 2021]. The flyby of a dwarf planet KBO (see definition below) will examine the potential for ocean world status through telltale characteristics that come from gravitational, compositional, and geological constraints.

Uranus had an intriguing early evolution that may have strongly influenced the origin of its regular satellites and their potential to be ocean worlds. An event occurring many billions of years ago tipped Uranus over on its side, giving it a spin axis nearly aligned with the ecliptic plane (obliquity of 98º). The satellites and rings of Uranus are all in its rotational plane such that we can deduce they formed after the Uranus tilting event.

A leading hypothesis regarding the origins of this tilt is that a giant impact occurred with Uranus; it potentially explains the planet's unusual spin state, as well as the ice- and rock-rich circumplanetary disk suitable for the formation of observed regular satellites and rings [e.g., Kegerreis et al. 2018]. This scenario suggests the close-in satellites of Uranus had a provenance unlike any other putative ocean world examined to date and, therefore, represents an unexplored frontier for planetary science.

KBOs have their own perplexing mysteries. Leading models indicate KBOs are ancient icy planetesimals and, as such, can reveal how the building blocks of the outer solar system planets were formed [Nesvorný et al. 2019; 2021]. They are believed to have accreted from tiny disk constituents called "pebbles" that were centimeters to decimeters in size. In the solar nebula,

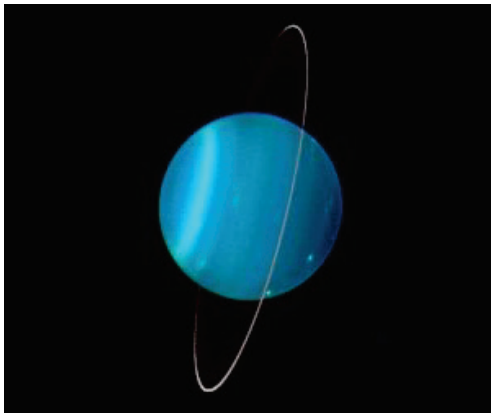

Exhibit 1-1. *The Uranian System is an intriguing destination in the search for ocean worlds. One hypothesis contends that Uranus's characteristic tilt was caused by an impact with a large, icy body – potentially explaining the configuration of its moon system, and could help explain the configurations of other icy planets in our solar system. Courtesy of: Lawrence Sromovsky, Univ. of Wisconsin-Madison/ W.W. Keck Observatory/NASA)*

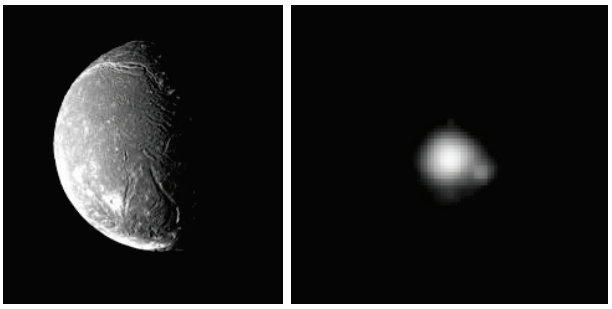

Exhibit 1-2. *Calypso baselines a mission that includes a flyby of Uranus, a close encounter with Ariel (left), then a close encounter with G!kún‖'hòmdímà and G!ò'é !Hú (right).*
Ariel image courtesy of: NASA Jet Propulsion Laboratory; G!kún‖'hòmdímà image courtesy of: NASA.

aerodynamic processes produced concentrations of pebbles. When these clusters achieved high enough spatial densities, they went through gravitational collapse into 100-km-class bodies [e.g., Nesvorný et al. 2019]. A common modeling outcome is that of well-separated, comparably sized bodies in orbit around one another. Such binary objects are relatively plentiful in the Kuiper belt, but details of how they formed await in situ study.

Once a KBO was created, it was subject to numerous collisions, possible internal processing, and dynamical upheaval [e.g., Tsiganis et al. 2005; Nesvorný & Morbidelli 2012; Nesvorný et al. 2016; Bierson & Nimmo 2019; Morbidelli et al. 2021]. By understanding the critical clues left behind on these bodies in terms of their compositions, spin states, shapes, geologic histories, and crater histories, we can potentially tell the history of planetesimal formation in the outer solar system, the evolution of the primordial Kuiper belt, and how this population was affected by the same giant planet migration events that reshaped the solar system.

Until recently, the conventional wisdom was that all but the largest such KBOs failed to experience sufficient heating via the decay of radiogenic isotopes to produce subsurface oceans. However, there are primitive objects in the asteroid belt that show attributes consistent with them having subsurface zones of weakness or muddy oceans that stretch to their deep interiors [e.g., Raymond et al. 2020; Vernazza et al. 2020; Carry et al. 2021]. According to current modeling work, these bodies likely formed in the giant planet zone and the primordial Kuiper belt [Walsh et al. 2011; Vokrouhlický et al. 2016]. The tantalizing prospect that dwarf planets in the Kuiper belt are actually ocean worlds could revolutionize our ideas of the nature of icy planetesimals, where they formed, how they evolved and the distribution of liquid water across the solar system. For these reasons, we have chosen to explore this class of KBOs with Calypso.

1.2 Calypso Baseline Mission

1.2.1 Uranian Moon Investigation

Many known or probable ocean worlds have been discovered across our solar system. Known ocean worlds like Europa and Enceladus have been confirmed through direct measurements and observations [e.g., Coustenis et al. 2020 and references therein]. The hypothesized presence of an ocean at Pluto in the Kuiper belt [e.g., Hussmann et al. 2006] would be the most distant liquid water reservoir discovered. An ocean deduced at Ceres, a 930-km body in the asteroid belt, may have a briny, muddy ocean, different from the salty liquid water reservoirs elsewhere [Castillo-Rogez et al. 2020].

The first half of the Calypso mission focuses on Uranian moons as possible ocean worlds. As discussed above, they may have formed as the byproduct of a giant Uranian impact. Any other origin scenario would need to produce a circumplanetary disk in the same rotation plane as Uranus after it had already been tipped over.

While there are several possible ocean words in the Uranian system that could be explored, the Calypso design concept must satisfy multiple goals:

1. The Uranian moon chosen should demonstrate promising geologic evidence that a subsurface ocean exists (from the available Voyager 2 images).
2. The KBO encountered should be approximately dwarf planet-sized – preferably larger than 400–600 km in diameter [Lineweaver & Norman 2010] – to maximize the probability that it is an ocean world. Here the most conservative diameter is used to select our targets.
3. The total time to reach a Uranian system ocean world and a dwarf planet KBO should be as short as possible to (i) maximize power from a radioisotope thermoelectric generator (RTG) over the entire voyage, (ii) maximize the probability that all spacecraft components will be in working order for all encounters in the nominal missions, and (iii) minimize mission costs.

When accounting for the aforementioned design goals, we find that the best moons to explore as ocean worlds are Miranda and Ariel. This determination is consistent with NASA's ROW, which prioritized Miranda and Ariel as the most likely ocean worlds in the Uranian system based on evidence for endogenic processes given the available data. From these two, Ariel was selected for our Calypso point design mission, with our rationale presented below. A discussion of our choice of a dwarf planet KBOs is provided in the § 1.2.2.

Note that our choice of Miranda and Ariel may represent observational bias, given that Voyager 2 captured the greatest number of high resolution images at Miranda and Ariel. Larger, more distant moons from Uranus are not as well characterized, although all moons show evidence of some endogenic-driven geologic processes [e.g., Schenk & Moore 2020]. For example, the size and hydrostatic state of the moons Titania and Oberon could be sufficient to contain oceans. Regardless, trajectories that take Calypso further from Uranus do not yield the same gravity assist opportunities as those closer to Uranus and, therefore, do not satisfy the time criterion as well as Miranda and Ariel.

Ariel Overview. Ariel was first seen by the Voyager 2 spacecraft in 1986 with image resolutions up to 1 km/pixel. Its surface, with smooth, flat-floored troughs and extensional faults, polygonal blocks separated by wide troughs (3-4 km deep), and relaxed craters shows evidence that its geologic history was dynamic [e.g., Schenk & Moore 2020]. The global distribution of extensional tectonics on a planetary surface can be used to determine whether they are related to the gradual freezing of a subsurface ocean. Planetary tectonics can also be used to infer the likelihood of fluid extrusion from an internal liquid layer onto the surface due to cryovolcanism. Estimates of elastic thicknesses are 3-4 km, and they suggest heat fluxes higher than can be accounted for from either radiogenic heat or tidal heating from Ariel's current eccentricity [Peterson et al. 2015]. Ariel's surface ages range from 1.4 ± 0.5 billion years old (Ga) for the more heavily cratered terrains to 0.8 ± 0.5 Ga for the smooth surfaces between polygonal blocks [Kirchoff & Dones 2018].

Ariel's dynamic array of geologic structures, combined with its possibly high heat fluxes, indicate that Ariel had a subsurface ocean in the past and possibly has a subsurface ocean today. We use this as a starting point to discuss Ariel's internal evolution.

Ariel's Interior Structure & Ocean Composition. Numerical models of Ariel's interior evolution show that volatiles accreted on the moon experienced substantial melting via short-lived radioisotope decay and/or tidal heating. These models are based on two interior evolutions reported in the literature:

- Differentiation of a mostly lithified rocky mantle and hydrosphere (ocean and icy shell) [e.g., Hussmann et al. 2006];
- Preservation of a porous, rocky mantle based on observations and models proposed for Saturn's moon Enceladus [Travis & Schubert 2015; Choblet et al. 2017; Neveu 2019].

Here we summarize predictions for Ariel's current thermal state and the prospect for the preservation of an internal ocean using the approaches by Neveu [2019] and Castillo-Rogez et al. [2019] (Ex. 1-3). These models assume that tidal heating has not been a major heat source in Ariel's recent past, given the combination of Ariel's relatively high eccentricity (e ~ 0.0012) (i.e., tidal forces should circularize Ariel's orbit) and its estimated youthful surface age of ~0.8 Ga [Schenk & Moore 2020].

For Ariel's Solid Mantle Model (Ex. 1-3), a wide range of thermophysical properties can be explored, with results leading to different levels of rock dehydration as a consequence of heat from long-lived radioisotope decay. These results lead to a range of hydrosphere thicknesses for Ariel of 170–255 km. For Ariel's Porous

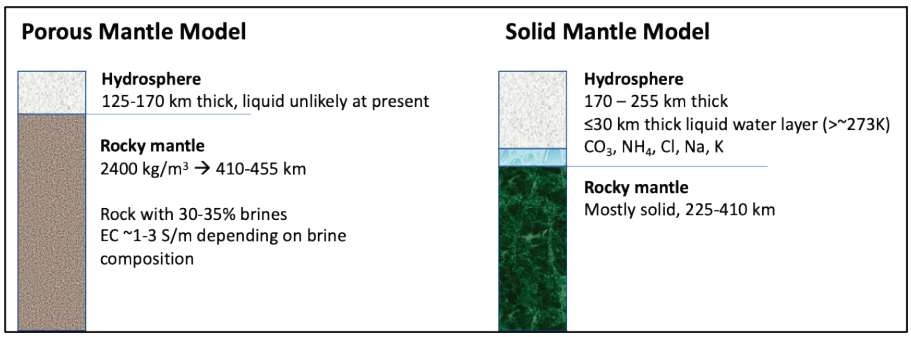

Exhibit 1-3. *Main characteristics of the interior models taken as a basis for computing the electromagnetic induction response of Ariel based after Neveu [2019] (left) and Castillo-Rogez et al. [2019] (right).*

Mantle Model Neveu [2019] chose a mantle density of 2400 kg/m^3 as derived for Enceladus [Iess et al. 2014], which is a relevant analog in terms of physical properties. These values yielded a hydrosphere thickness of 125–170 km, where the spread comes from the uncertainty in Ariel's mean density.

Both models allow for the formation of clathrate hydrates as the hydrosphere freezes that can explain the preservation of subsurface liquid at Ceres and Pluto [Castillo-Rogez et al. 2019; Kamata et al. 2019]. In absence of clathrate hydrates and tidal heating, the hydrosphere freezes on a timescale of about 100 Mya for all models. The addition of a large fraction of clathrates leads to the preservation of a residual ocean up to ~30 km thick in the Solid Mantle Model. For the Porous Mantle Model, brines in the mantle can be preserved until the present day, with Ariel's ocean residing below a frozen hydrosphere and over a mantle diameter of ~430 km.

Ocean salinity is a critical factor in deciding whether an induced magnetic field within Ariel's putative ocean can be detected by Calypso's magnetometer. Our estimates of this value come from new work by Castillo-Rogez et al. [submitted], which makes several assumptions:

- Differentiation, and subsequent concentration, of salts in the remnant liquid as a consequence of freezing within the interior.
- Volatile concentrations are based on cometary and recent cosmochemical models [e.g., Mousis et al. 2020]. The role of supervolatiles (e.g., CO_2, NH_3, CH_3OH) accreted in the form of ices is also included.
- The modeling approach builds on previous studies that identified the role of carbonate ions as major solutes in, e.g., Enceladus [>0.5-2 wt.%, Postberg et al. 2011; Glein & Waite 2020] and Ceres [Carrozzo et al. 2018; Castillo-Rogez 2020].

Castillo-Rogez et al. [submitted] show that an average cometary composition of [CO]+[CO_2] ~4 wt.% and [NH_3] ~0.3 wt.% of accreted volatiles leads to a salinity >1 wt.% prior to concentration (i.e., assuming all the water is in liquid form). For a solution dominated by Na^+, HCO_3^-, NH_4^+, Cl^-, CO_3^{2-}, this corresponds to an electrical conductivity (EC) about 1.5 S/m at 0°C and 1 bar [McCleskey et al. 2012].

EC increases upon solute concentration in the ocean as a consequence of shell freezing. In a residual layer of <10 km, the solution is saturated in chlorides. For ionic strength (above 1 mol), we rely on analog and laboratory studies to constrain the EC of hypersaline solutions [e.g., Rebello et al. 2020]. Waters with salinities similar to those obtained for Ariel reach conductivities of about 23 S/m, computed for a reference temperature of 25°C.

Based on empirical temperature correction factors [Smith 1962], an EC of 23 S/m at 25°C translates to an EC of ~15 S/m at 0°C for the Solid Mantle Model. We consider this a lower bound on EC because pressure tends to increase EC at pressures of tens of MPa relevant to Ariel's residual ocean [Schmidt & Manning 2017]. Besides, the residual liquid layer trapped between insulating layers of precipitated chlorides and clathrate hydrates is likely warmer than 0°C [see related work by Kargel et al. 2005 for Europa].

In the case of the Porous Mantle Model, the EC of the mixture computed with Archie's law is of the order of 1–3 S/m for 30% brine mixed with rock (the range covers uncertainties in brine temperature).

We will use these salinity values in the next section when we discuss detectability of an ocean using Calypso's magnetometer.

Ocean Detection at Ariel. Calypso employs the classic technique of magnetic induction to search for conducting subsurface saltwater oceans [Parkinson 1983, Zimmer et al. 2000]. Time-varying fields inside a conducting body generate currents by Faraday's law of induction. These currents, in turn, generate a secondary magnetic field by Ampere's Law that can be sensed by a magnetometer.

Uranus's magnetic field is well described by a dipole offset by ~0.3 of its radius along the spin axis toward the north pole and tilted by 59° [Connerney et al. 1987]. The wobbling of this dipole, due to the rotation of Uranus and orbital motion of Ariel, produces a time variable field in the reference frame and location of Ariel. In particular, using the internal hexadecapole AH_5 magnetic field model from Voyager 2 data Herbert et al. [2009], Weiss et al. [2020, 2021], and Cochrane et al. [2021] found that the dominant frequency at Ariel is the 24-h synodic frequency with an amplitude of ~100 nT.

This driving field can be used to probe for the subsurface ocean similar to the two structures described in the previous section. To assess this possibility, following Weiss et al. [2020, 2021], we calculated the induced field during a Calypso flyby assuming a spherically symmetric body with a rocky interior overlain by conducting

ocean and capped with a nonconducting ice shell. For a single flyby within ~450 km altitude of the surface, we find that both types of oceans should produce induced surface fields with amplitudes exceeding the typical ~1 nT sensitivity of spacecraft magnetometry investigations (Ex. 1-4).

Bonus Science from Calypso in the Uranian System. Calypso's comprehensive payload will have the opportunity and ability to complete complementary science investigations. Calypso's imaging capability will obtain near-global image and compositional coverage of Ariel when combined with low-resolution images from Voyager 2. Calypso will also obtain similar coverage of the remaining four regular Uranian moons, providing the scientific community with additional data to infer whether a subsurface ocean existed or currently exists at each of these moons.

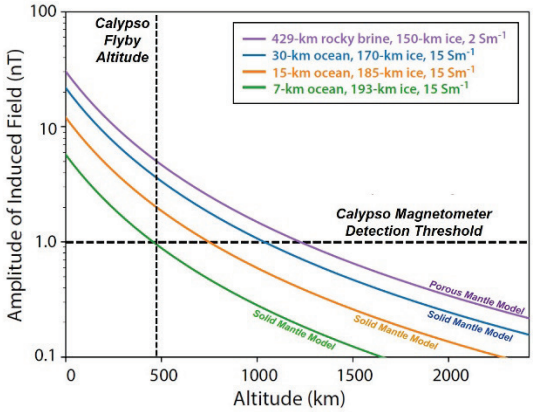

Exhibit 1-4. *Predicted induced magnetic fields from subsurface oceans in Ariel during a Calypso flyby. Curves denote the amplitude of the induced field as a function of distance from the induction pole on the surface. Purple curve denotes induced field for 429-km rocky brine with conductivity of 2 S m^{-1} overlain by 150-km thick ice layer (Porous Mantle Model). Blue, orange, and green curves denote induced fields for water oceans with conductivities of 15 S m^{-1} and fixed H_2O thickness of 200 km: 30-km ocean overlain by 170-km thick ice (blue), 15-km ocean overlain by 185-km thick ice (orange), and 7-km ocean overlain by 193-km thick ice (green) (Solid Mantle Model).*

The Calypso payload will also support additional science in the Uranian system during its flyby. In-situ sampling of the plasma, energetic particles, and magnetic field upstream of, and within, the Uranian magnetosphere will provide bountiful information on this vastly under-sampled system. In particular, Calypso will encounter Uranus just prior to its spring equinox, providing additional data points of its magnetic field, topology, and solar wind coupling to compare and contrast to those from the 1986 Voyager 2 flyby, possibly revealing information on potential seasonal variations. Further, the combination of Calypso's scientific payloads and trajectory will enable novel measurements of the composition of suprathermal ion population left unsampled by Voyager 2, which may provide important clues to the causation of the Uranian magnetosphere and the source of the planet's surprisingly intense electron radiation belts, which are at their most intense near the orbit of Ariel.

Finally, Calypso can survey Uranus's system of rings and small moons on approach, providing information about their compositional variations and, perhaps, lead to the discovery of additional small moons. After passing by the planet, the spacecraft is expected to provide the first clear view of Uranus' complex system of dusty rings since Voyager.

1.2.2 Dwarf Planet KBO Investigation

The Kuiper Belt is a rich area for scientific investigation and can be considered one the final frontiers of our planetary system. Its exploration has important implications for better understanding comets, solar nebula (and extra-solar disks), the origin of small worlds, and the solar system as a whole. It can also tell us how primitive material from the planet formation era has evolved thermally in different solar system zones.

KBOs are thought to be primitive, volatile- and organic-rich planetesimals. They are of key scientific interest because they are effectively the leftovers of giant planet formations and, thus, provide a fossil record of the outer solar system. In many ways, KBOs hold the key to answering fundamental origins questions, such as *"How are planetary systems born and how do they evolve?"*

Numerical simulations indicate that the present-day Kuiper belt is a relic of a massive primordial planetesimal population that once stretched from ~20–50 AU [Tsignais et al. 2005; Nesvorný et al. 2016; 2018]. This population was depleted possibly by a factor of 1000 when the original orbital configuration of the giant planets went unstable. The exact timing of this event is still unknown but led Uranus and Neptune to migrate through the primordial Kuiper belt. Events triggered by this process fundamentally changed our solar system and helped define our system of planets, satellites, and small body reservoirs.

The largest KBOs that survived the giant planet migration can be categorized as dwarf planets. As suggested by the New Horizons exploration of the Pluto system, some may host their own satellite systems. It is also

likely that some dwarf planets have experienced geological processes, surface frosts, sporadic atmospheres, and internal oceans. It is the last subject that will be of particular interest to the Calypso mission, with recent work favoring such worlds as plausible candidates to have subsurface oceans (see below).

Choice of Dwarf Planet Target. The trajectory studies discussed below indicate that Calypso can plausibly visit one of many different dwarf planet targets. The number of dwarf planets available to visit depends on variables such as (i) launch time, (ii) the choice of Ariel or Miranda as a target for a close flyby within the Uranian system, (iii) mission length, and (iv) size threshold for dwarf planets, (here we have assumed $D \geq 600$ km to satisfy a conservative dwarf planet criterion; [Lineweaver & Norman 2010]). Examples of possible dwarf planet target scenarios investigated by our team include:

- Launch times in 2033–2036 that can take advantage of a gravity assist from Jupiter (JGA) to encounter Ariel/Miranda. This allows Calypso to reach (229762) G!kún‖'hòmdímà, (19521) Chaos, (20000) Varuna, or (208996) 2003 AZ84 in 17–21 years.
- Launch times in 2030–2032 that do not use a JGA. Instead, Calypso assumes a "Uranus Direct" trajectory to Ariel/Miranda, with launch energies comparable to that of New Horizons. Under these conditions, Chaos and Varunua can be reached in 15–19 years.
- Launch times in 2040–2042 that assume a Uranus Direct mission to Ariel, Varunua, and (208996) 2003 AZ84 can be reached in 16–19 years.

All of these targets have additional intriguing attributes that would make excellent targets to not only test the limits of ocean worlds, but also explore various KBO formation and evolution scenarios. For example:

- (208996) 2003 AZ84 and (229762) G!kún‖'hòmdímà both have satellites (see references at http://www.johnstonsarchive.net/astro/asteroidmoons.html).
- (20000) Varuna has an elongated shape due to its rapid rotation and may have a close-in satellite [e.g., Fernandez-Valenzuela et al. 2019].
- (19521) Chaos shows no measurable short-term photometric variations in the timescales of hours, and that could mean it has a long rotation period over days [Sheppard & Jewitt 2002, Lacerda & Luu 2006]. If true, one possible explanation is that Chaos was born with a satellite that removed most of the rotational angular momentum via tides [Nesvorný et al. 2019, 2020b]. This putative satellite would have been stripped during Chaos's early evolution by collisions or an encounter with Neptune. Chaos has also had water ice reported in its spectral signature [Barkume et al. 2008], though follow-up observations suggested its spectrum may resemble that of other KBO spectra [Brown et al. 2012].

For our baseline study, we chose a target KBO for Calypso to minimize mission length and remain within the 2033–2036 launch window time frame. This led us to (229762) G!kún‖'hòmdímà and its satellite G!ò'é !Hú.

G!kún‖'hòmdímà Overview. G!kún‖'hòmdímà and G!ò'é !Hú (pronunciation GOON-hohm-DEE-mə and GOH-ay-HOO) are names from Namibian mythology. Phonetic characters (!, |, ‖) correspond to click consonants, and vowel markers (´,`) correspond to high and low tones in the conventional spelling system of the Ju|'hoan people native to ingenious to parts of Namibia and Botswana.

Like most KBOs, only a few of the properties of G!kún‖'hòmdímà-G!ò'é !Hú have been well characterized. Its orbit makes it a member of the extended scattered disk. This population was created during Neptune's migration, where objects residing in a disk-like primordial Kuiper belt were scattered outward by Neptune [e.g., Gomes et al. 2008]. This event left the binary with a semi-major axis, eccentricity, and inclination (*a, e, i*) values of (72.8 AU, 0.484, 23.4°), respectively. Objects in the extended scattered disk can no longer encounter Neptune, so G!kún‖'hòmdímà-G!ò'é !Hú provide us with a preserved record of what happened to the primordial Kuiper belt during Neptune's migration through it.

Observations indicate the diameter of G!kún‖'hòmdímà is $678.0 \pm 11 \times 611.4 \pm 18$ km, larger than all main belt asteroids except Ceres [Grundy et al. 2019, Schindler et al. 2017, Benedetti-Rossi et al. 2016, Thirouin et al. 2014]. The combined mass of the binary is 1.36×10^{20} kg, and that yields a bulk density for G!kún‖'hòmdímà near 1 g cm^{-3}. For reference, both values are comparable to Saturn's moon Enceladus. The estimated albedo of G!kún‖'hòmdímà is 0.15.

The size ratio between G!kún‖'hòmdímà and G!ò'é !Hú is estimated to be 4.45, giving G!ò'é !Hú an estimated diameter of 150 km. More puzzling are the colors and orbit of G!ò'é !Hú. G!ò'é !Hú happens to be one of the

reddest known KBOs, unlike G!kún‖'hòmdímà, which suggests a possible capture origin. One potential issue with this scenario is that G!ò'é !Hú has a relatively close, nearly-circular orbit (a = 6078 km, or roughly 20 times the radius of G!kún‖'hòmdímà, and e = 0.0236±0.0066). In many ways, this makes the system comparable to a scaled version of the Pluto-Charon system. Accordingly, the G!kún‖'hòmdímà-G!ò'é !Hú binary may provide insights into the dynamical or possibly collisional mechanisms that produced that system.

The flyby of the G!kún‖'hòmdímà-G!ò'é !Hú binary will take place at a speed of 9 km/sec at a likely distance of several thousands of kilometers. This will allow Calypso to obtain high-resolution imaging and imaging spectroscopy which, in turn, will be used for geology, geophysics, and compositional studies. Observations on approach to G!kún‖'hòmdímà-G!ò'é !Hú will help determine the shape, rotational periods, and orbits of G!kún‖'hòmdímà and G!ò'é !Hú. They will also facilitate studies of both the heliospheric plasma (solar wind, pickup ions, and energetic particles) and dust environment that G!kún‖'hòmdímà-G!ò'é !Hú orbits in, and they will enable the search for both satellites and rings at resolutions and sensitivities not otherwise achievable.

At its closest encounter of the binary system, Calypso will map the surfaces of G!kún‖'hòmdímà-G!ò'é !Hú in both panchromatic and color channels, map their detailed 3D shapes and topography, map photometric properties across their illuminated surface, map its surface composition, measure day- and night-side temperatures, and search for evidence of volatile escape, coma, and other surface activity.

G!kún‖'hòmdímà as an Ocean World. The Calypso flyby of G!kún‖'hòmdímà-G!ò'é !Hú offers a window on the formation and evolution of objects that test the limits of ocean worlds. On the one hand, the ~600 km body G!kún‖'hòmdímà has spent its life in a deep freeze, and the prospects for extensive early heating seem limited. On the other hand, several bodies in the main asteroid belt thought to be captured from the outer solar system [Walsh et al. 2011; Vokrouhlický et al. 2016] appear to show evidence that they may have subsurface oceans.

For example, consider (1) Ceres, a 930 km carbonaceous chondrite-like body that likely formed in the giant planet zone [De Sanctis et al. 2015]. It shows evidence for cryovolcanism, subsurface brines that have reached the surface, and a curious paucity of large impact basins that should have been produced by impact with large main belt asteroids over 4.5 billion years [e.g., Marchi et al. 2016; Raymond et al. 2020]. The latter could be explained by a subsurface zone of weakness that would permit large basins to undergo viscous relaxation.

As a second example, consider (10) Hygiea, the fourth largest main belt asteroid with a diameter > 400 km. It was hit by a very large asteroid in the past, an event that produced a substantial number of fragments. Observations of Hygiea with VLT/SPHERE, however, show it is nearly a perfect sphere, with no obvious evidence of any large impact scar [Vernazza et al. 2020]. This outcome again suggests substantial viscous relaxation of large scale surface topography and a sub-surface ocean. These examples bracket the size of G!kún‖'hòmdímà, and other examples like them in the literature, such as (87) Sylvia, a 270-km irregularly-shaped asteroid with J_2 values suggesting a subsurface ocean [Carry et al. 2021], indicate G!kún‖'hòmdímà may, indeed, be an ocean world.

The ability to deduce an ocean within G!kún‖'hòmdímà will rely on geological analysis via imaging and spectral signatures. Does this world have faults or other features that would suggest an ocean slowly freezing over time? Does it show evidence for cryovolcanism, brines brought to the surface, or viscously relaxed basins? Does it show compositional variation across its surface? Our expectation is that geologic evidence of ocean evolution may be preserved on KBO surfaces and can be used to infer details on their interiors.

Extended Mission Target Possibilities for Calypso in the Kuiper Belt. Like New Horizons, Calypso has the potential to visit additional not-yet-discovered KBOs along its trajectory. Calculations using the Canada-France Ecliptic Plane Survey (CFEPS) L7 model [e.g., Kavelaars et al. 2009] by A. Parker [personal communications] suggest that there are ~18 KBOs with D > 20 km per $(AU)^3$ between 40–50 AU. This size is comparable to the mean diameter of Arrokoth, and it is close to the observational limit of the Hubble Space Telescope (HST) in that zone of space.

We also estimate that the volume of space that Calypso could reach between 40–50 AU (in an expanding cone) is 0.09 $(AU)^3$. Multiplying the two values, we find Calypso could reach an additional ~1–2 KBOs with D > 20 km. If telescopic assets more powerful than HST become available over the next several decades, even more encounters with smaller KBOs will be discovered within this encounter volume.

Accordingly, we anticipate that the Calypso mission could potentially visit additional small KBOs prior to the end of its lifetime. Such encounters could help us better understand the origin and evolution of both the Kuiper belt and smaller KBOs in general.

1.3 Science Objectives & Science Traceability

Calypso provides a mission concept with a rich set of targets that stands to transform our understanding of ocean worlds. Other compelling reasons for Calypso include:

- The Uranus system has not been visited since Voyager 2, and impact-generated moons are arguably the "final frontier" of ocean worlds;
- KBO exploration has barely begun, and intriguing dwarf planets like G!kún‖'hòmdímà may hold the key to numerous solar system origin questions; and
- Uranus is perfectly positioned to allow us to visit large KBOs from now to the 2040's, without having to rely solely on a JGA as a prerequisite.

The importance of revealing the distribution and history of liquid water reservoirs across our solar system is one of the most prominent pillars in our search for extant life. Two primary goals drove the Calypso study:

1. **Ocean world system science.** Calypso's flybys are optimized for a robust induction measurement at an ice giant satellite. Imaging of an ice giant moon and distant planetesimal will help us identify and characterize their global geologic history and surface compositions. Calypso's suite of heritage instruments combine to make Calypso a deep space observatory tailor-made for ocean detection and environmental science that will collect imagery on the remaining unmapped regions of an ice giant moon and potentially reveal a new dwarf planet system in the solar system.
2. **Architecture rich with targets and launch opportunities.** Calypso's robustness is non-specific; the science objectives for the Ariel and G!kún‖'hòmdímà flybys are achievable at other ice giant moons and dwarf planets with the same payload.

The major science goals for the Uranian moon flyby portion of the mission are as follows, with specific tie-ins to our baseline visit to Ariel.

Search for Ariel Subsurface Ocean and Internal Structure. Uranus's magnetic field is expected to induce a magnetic field signal if a salt-rich ocean resides within Ariel. By performing this measurement during a close encounter 450-km above the moon's surface, Calypso will detect and characterize the elements of a putative ocean. A negative detection of an induced magnetic field will be robustly determine the lack of an ocean, a result that will deepen our understanding of the limits on ocean worlds. Furthermore, Calypso will image Ariel's northern hemisphere at sub-km resolutions and provide near global coverage of Ariel when combined with existing data collected from the Voyager 2 mission, revealing a complete picture of the moon's dynamic geologic history. In addition, surface geology is strongly connected to changes in a world's interior. By combining geologic information with Calypso's magnetometer measurements, Calypso will test whether Ariel is an ocean world, and will determine where it fits in the family of past and/or present ocean worlds.

Voyager 2 did not obtain any compositional information at Ariel, but ground-based observations have detected strong CO_2 ice bands on its surface [Grundy et al. 2003; 2006]. Current best estimates of the sources of these bands are radiolysis by magnetospheric particles [Grundy et al., 2006], however there may also be a direct link between geologic activity and the presence of CO_2 on the Uranian moons. Compositional mapping across Ariel can uncover links to geological processes potentially reveal subsurface-surface exchange processes, and provide clues to Ariel's origins and formation.

Characterize crater populations. Ariel has a rich crater history that contains both ancient and relatively fresh geological units. The best age estimates for Ariel's observed ancient terrains are 1.4 ± 0.5 Ga [Kirchoff & Dones 2018], but still older terrains may yet be imaged. The younger units (smooth terrains 0.8 ± 0.5 Ga [Kirchoff & Dones 2018]) should characterize the nature of the cometary impactors striking from the scattered disk over the last several billions of years [Gomes et al. 2008]. Changes in the crater size distribution, potentially produced by secondaries and sesquinaries, may also be observed on different terrains [Schenk & Moore 2020]. We will characterize the relative timing of events on Ariel, probe the evolution of the Kuiper belt and scattered disk, and will estimate the absolute model ages of the oldest terrains on Ariel. In turn, this will allow us to glean insights into the full history of Ariel. We point out that comparable studies can be completed for all of the imaged Uranian satellites with Calypso's payload and flyby architecture.

Uranian System Science: Uranus, Rings, Ring-Moons, and Satellites. The Uranian system has not been imaged since Voyager 2, and studies of Uranus, its rings, ring-moons, and other satellites will provide a deluge of information about how ice giant systems have evolved.

The major science goals for the KBO/dwarf planet flyby portion of the mission are as follows, with specific tie-ins to our baseline visit to G!kún‖'hòmdímà and G!ò'é !Hú.

Characterize the global geology and morphology of G!kún‖'hòmdímà/G!ò'é !Hú and their rotational and physical properties. The geology, rotational, and physical properties of the dwarf planet G!kún‖'hòmdímà and its satellite G!ò'é !Hú are expected to reveal critical clues about their origin and evolution. Additional constraints will come from a comparison between the binary's landforms and regolith and those of comets, asteroids, and icy satellites. The overall shapes of the primary body and its satellite will be a key constraint on planetary accretion models, as well as on possible giant impact/satellite capture models that have occurred post-accretion. Calypso will collect imagery to search for geologic and regolith units. The relative ages of different surface units will be determined by the spatial variation in crater populations.

Calypso will also search for layering on exposed scarps, crater walls, and other topographic features for clues to the origin of the binary, to search for evidence of interior or surface fragmentation, and to search for evidence of surface and interior evolution, including possible volatile loss. Fracture patterns and derived topography will be used to constrain internal strength and history.

Map surface composition and volatile distribution. Studies of the binary's color and composition will illuminate the thermal and compositional environment. They will also allow us to glean insights into the nature of the material from which it was assembled, radial mixing in the nebula, and the evolution of the surface of each binary component. Because of its long-term cold storage, some fraction of G!kún‖'hòmdímà and G!ò'é !Hú constituents may have survived little altered from icy pebbles and gases from the protosolar nebula. We expect solids resulting from varying degrees of thermal processing, potentially including sublimation and condensation of some volatiles but not others.

Calypso observations will identify sub-units across each binary component by searching for differences in their visible colors and detecting their infrared absorption features. In addition to searching for surface color and composition variegation, Calypso will also use craters as windows into the interiors of both bodies. These various studies may also shed light on the puzzling color diversity of KBOs in general. Accretional history may be particularly evident if G!kún‖'hòmdímà and G!ò'é !Hú were brought together by a Pluto-Charon-style impact capture event because materials exposed may tell us about the internal compositional and physical structure of each body.

Characterize crater populations. Crater populations will be used to constrain the collisional history of the primordial and present-day Kuiper Belt. The primordial Kuiper belt was perhaps 1000 times larger than the observed population such that early collisional evolution would have been extreme [Nesvorný et al. 2019; Morbidelli et al. 2021]. From there, giant planet migration would have scattered most of the population, leaving the Kuiper belt close to its current mass and dynamical state. During this period, the size distribution of KBOs would have been changing rapidly in response to collisions. G!kún‖'hòmdímà would have seen an integrated version of the full impact history of the Kuiper belt. By combining crater constraints with numerical models of the collisional and dynamical evolution of the Kuiper belt, it will be possible to explore its history and estimate the timing of when giant planet migration was initiated, a critical component for determining the full history of our solar system.

Search for satellites and rings. Calypso will search for rings and additional satellites during each encounter. If detected, Calypso would provide the first close-up observations of small body ring systems, potentially providing key information on the formation and evolution of these puzzling structures.

Ex. 1-5 maps the science objectives at each flyby target in order of their priority level (1, 2, or 3). Calypso's threshold mission will achieve each of these science objectives. Each science objective is achieved by the science measurements, technical requirements, and the instrumentation needed to complete these measurements. Calypso's comprehensive 10-instrument payload (9 unique) satisfies the science objectives laid out in the traceability matrix. Calypso's payload will achieve the same science objectives across a variety of other trajectories, and can include alternate ice giant satellites and different large (≥600km) KBO targets.

Exhibit 1-5. *Science Traceability Matrix. Note: objectives assume a binary KBO; adjustment may be required if a target other than G!kún‖'hòmdímà is selected.*

Priority	Science Objective	Measurement Obj	Measurements	Instruments	Mission Rqmts	Comments
Uranian Moon Investigation						
1	What is the internal structure? Does Ariel have an ocean? Does Ariel have an internal magnetic field?	Gravity field, magnetic field, moment of inertia	B-field from induction, dynamo or remnant magnetization, moment of inertia, 1 nT signal measured at 0.3 nT resolution	MAG, NAC, RS, E-ESA, I-ESA	fly close to a Uranian moon, preferably Ariel, before or close to 2049	Gravity field by standard S/C ranging. Contributing measurements from plasma instrument.
1	What geological history and processes do the surfaces record? What processes contribute to surface-subsurface exchange? Have there been active processes in the geologically recent past?	Global map of highest achievable resolution, given flyby timing	Northern hemisphere coverage images with < 1 km/pix surface resolution for geomorphic mapping; stereo and/or lighting to ascertain topography, regional (north and/or south) image resolution <300 m/pix for stratigraphy of units; panchromatic & color	NAC, Vis/NIR MVIC	fly close to a Uranian moon, preferably Ariel, before or close to 2049	
1	What is the composition of surface materials? How are volatiles distributed? What are the ranges of surface temperatures? Is the red material on the moons' surfaces organic-rich and what is its provenance?	Surface ices and mineral maps; temperature map	Global NIR spectral map with resolution <1 km/px; global thermal map with 4-channel color, 0.4-0.55, 0.54-0.7, 0.78-0.97, 0.86-0.91 (methane) μm. >250 channels hyperspectral 1.25-2.25 μm at <3 km/px baseline	Vis/NIR LEISA; & MVIC, UVIS	fly close to a Uranian moon, preferably Ariel, before or close to 2049	UV and thermal mappers are lower priority on the payload
2	Is there evidence on multiple moons for a catastrophic event associated with Uranus getting tilted? Do we see evidence for extreme tidal heating, now or in the past?	Global map of surface at highest achievable resolution, given flyby timing	Northern hemisphere coverage images with < 5 km/pix resolution for crater counts; stereo and/or lighting to ascertain topography, regional (north and/or south) image resolution <3 km/pix for stratigraphy of units; broadband color	NAC, Vis/NIR MVIC	fly close to a Uranian moon, preferably Ariel, before or close to 2049	
3	How is the surface affected by the impingement of Uranian magnetospheric plasma?	UV albedo map; characterization of plasma impinging on surface	Approach and look-back images <200 km/px, 46.5-188 nm. Near-approach <5 km/px.	UVIS; EPD, E-ESA; I-ESA, MAG; D-Count	fly close to a Uranian moon, preferably Ariel, before or close to 2049	UV and thermal mappers, dust counter are lower priority on the payload
KBO/Dwarf Planet Investigation						
1	What is the internal structure of the primary? Does it have an ocean and/or an internal magnetic field? What is its bulk composition? What are the main rotational and physical properties of the primary and its satellite?	Bulk properties, gravity field, magnetic field, moment of inertia, rotational period, spin poles, and shape of both component.	B-field signature, moment of inertia, period/rotation.	MAG, NAC, HGA (Doppler tracking)	fly within 10,000 km of a dwarf planet and its satellite	The satellite is too small for an ocean
1	What geological history and processes do the surfaces record? What processes contribute to surface-subsurface exchange for the primary? Have there been active processes in the geologically recent past, especially for the primary? What are the crater counts on the primary and its secondary and can we infer the terrains ages?	Global map of surface at highest achievable resolution, given flyby timing	Hemispheric coverage images with <1 km/pix resolution for geomorphic mapping; stereo and/or lighting to ascertain topography, regional image resolution <300 m/pix for stratigraphy of units; broadband color	NAC, Vis/NIR MVIC	fly within 10,000 km of a dwarf planet and its satellite.	
1	**For both objects:** What is the composition of surface materials? How are volatiles distributed? What are the ranges of surface temperatures? Are there any surface heterogeneities/albedo spots? **For the primary**: Does the primary have a (tenuous) atmosphere?	Surface ices and mineral maps; temperature map; atmospheric pressure and composition; haze layers	Global NIR spectral map with resolution <1 km/px; global thermal map with 5-channel color, 0.4-0.5, 0.5-0.625, 0.625-0.75, 0.75-0.975 0.86-0.91 (methane) μm. >550 channels hyperspectral 1.0-3.6 μm at <3 km/px baseline	Vis/NIR LEISA & MVIC, UVIS, RS	fly within 10,000 km of a dwarf planet and its satellite.	UV and thermal mappers are lower priority on the payload
2	Are there additional moon(s) and/or rings/debris? Was the known moon (G!ò'é !Hú) captured or formed by collisions or did the system evolve in situ via tides? In case of additional moons, what are their rotational and physical characteristics and were they captured, formed by collisions or other? In case of rings/debris, what are their main properties (composition, size) and how did they form?	Images of system inbound and outbound to look for moons, rings and dust	Approach and look-back images <5 km/pix; spectral characterization to support imaging	NAC, Vis/NIR MVIC	fly within 10,000 km of a dwarf planet and its satellite.	
3	How is the surface/atmosphere affected by the impingement of the solar wind?	UV albedo map; characterization of plasma impinging on surface	Hemispheric coverage <1 km/pix, 46.5-188 nm	UVIS; EPD, E-ESA; I-ESA, MAG; D-Count	fly within 10,000 km of a dwarf planet and its satellite.	UV and thermal mappers, dust counter are lower priority on the payload

2. High-Level Mission Concept

2.1 Overview

The success of New Horizons demonstrated the effectiveness of flyby missions to collect scientific observations of distant worlds within the cost-conscious parameters of a New Frontiers-class mission. Calypso builds upon the flight-hardened experience of New Horizons, leveraging a proven spacecraft design and mission concept for another exciting journey of scientific discovery in the outer solar system.

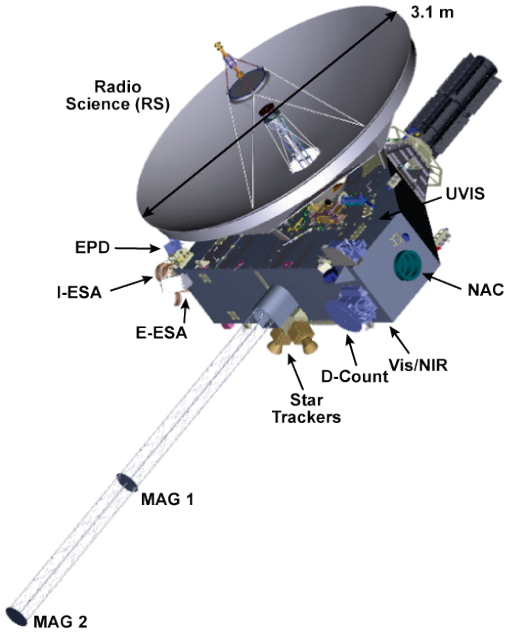

Exhibit 2-1. *The Calypso spacecraft has been expanded from New Horizons to accommodate a larger high-gain antenna and propellant tank. Its instruments all have strong heritage.*

The Calypso spacecraft is capable of both Spinning and 3-Axis modes, which enable peak power modes for science gathering and data downlink to be sequenced such that the mission requirements are met by a single RTG power source. The structure of the spacecraft has been expanded from New Horizons to accommodate a larger 3.1-m high-gain antenna (HGA) and propellant tank. A 4-m open lattice deployable mast boom with two equidistantly affixed magnetometers has been added to support magnetic induction observations. The selection and placement of Calypso's payload instruments were heavily informed by those flown on New Horizons based on similarities in the capabilities required to meet all science objectives. Each instrument included in the design has a TRL of 8 or higher and will have been flown on a prior mission ahead of Phase B. The 2035 launch date was chosen from the mission design trades for its favorable pass through the Uranian system, which provides multiple opportunities to collect new data and observations of previously uncharted surface regions of Uranian system bodies, including Ariel. At the time of the first encounter, G!kúnl'hòmdímà will be within 10° of the Uranus ecliptic plane, minimizing the ΔV required for the post-Ariel orbit correction maneuver and saving propellant for the extended mission.

Calypso will launch on a Falcon Heavy Expendable vehicle (or equivalent) between 11–31 Jul 2035. Coupled with a Star 48BV-powered kick stage, the spacecraft will be placed directly into its JGA transfer orbit toward the Uranian system with a maximum launch energy of 121 km^2/s^2, enabling the spacecraft to arrive at G!kúnl'hòmdímà after 17.1 years in flight. Following launch, the in-flight system checkouts will include the one-time deployments of instrument aperture covers and the magnetometer boom. Thereafter, the spin balance mechanisms will be used to align the HGA boresight with the principle spin axis. Next, the spacecraft's plasma and particle instruments will be brought online and will make continuous observations for the entirety of the mission (as power levels afford).

On 16 Nov 2036, Calypso will increase its heliocentric speed to 21 km/sec as it passes by Jupiter at a range of 1.7 million km, 494 days after launch. Following the gravity assist, the spacecraft will be placed into Hibernation mode in which many of the onboard components will be powered off to maximize component lifetimes and minimize operational costs. The operations team plans to awaken the spacecraft during its cruise phase to conduct an in-flight rehearsal of the flyby sequence. As the spacecraft nears Uranus, it will begin the Approach Observatory Phase (AOP) for the flyby where it will begin using its panchromatic narrow-angle camera at regular intervals to fine-tune the orbit determination solution and navigate to the reference trajectory. A few days ahead of the Ariel encounter at a distance of about 1 million km, the high-resolution cameras will begin collecting panchromatic and color images of Uranus, its rings, and several of its moons.

On 1 Nov 2041, Calypso will proceed towards Ariel from its northern hemisphere, targeting a flyby altitude of 450 km at a speed of 15.2 km/sec. The spacecraft will enter a slow rotation about its spin axis with the HGA

pointed towards Earth before inhibiting its thrusters for the 30 min centered on the point of closest approach, during which time the critical magnetic induction and radio science gravity observations will take place. Additional surface mapping may be attempted at the time of closest approach, though requirements will be met prior to the magnetometer and gravity measurements. Three-axis attitude control will resume thereafter while Calypso conducts targeted high-phase look-back observations to study magnetospheric plasma prior to the spacecraft's departure towards G!kún‖'hòmdímà. Calypso will target a close approach of G!kún‖'hòmdímà on 9 Sep 2052 at an altitude of 1,000 km and a speed of 9.1 km/sec. Observations similar to those conducted during the Ariel encounter will be made of the KBO and its moon with additional science objectives dedicated to studying the formation of this unique binary system. Unallocated ΔV and power margins estimate that an extended mission beyond G!kún‖'hòmdímà is feasible, and that at least one KBO greater than 20 km exists within the reachable volume of this ΔV.

2.2 Concept Maturity Level (CML)

The Calypso mission concept has been developed to CML-4 as a preferred design point. The proposed spacecraft design includes details to the subsystem level, with 30% margin for mass and power as defined by the PMCS guidelines. Cost, schedule, and risk assessments were conducted and are shown to fall within acceptable ranges as outlined by the PMCS guidelines. Trades were conducted against the baseline science mission to provide alternative options for the proposed launch date and trajectory design. The threshold science is defined as all of the Priority-1 science objectives, representing the performance floor for the mission. As is often the case, the payload instruments selected to meet Calypso's Priority-1 requirements are capable of achieving more return than that of the threshold mission science..

2.3 Technology Maturity

Calypso leverages a similar spacecraft bus to that of New Horizons, with minor design enhancements to accommodate a larger 3.1-m HGA and a 4-m magnetometer boom. The instruments tasked with conducting scientific measurements and observations at each encounter are all heritage payloads that have either flown on prior missions or are currently in development for missions that will fly prior to the Calypso launch. All components are greater than TRL 6, with several being at TRL 8.

2.4 Key Trades

After selecting the Uranian system as the preferred destination for this mission, the trades conducted for this concept study centered on the mission design parameters required to reach the system within the estimated timeframe of a New Frontiers program. Targeting an optimal launch date in the 2033–2035 timeframe, the transfer trajectory options considered were a Direct-to-Uranus, a JGA-to-Uranus, and a 3-year ΔV-Earth-Gravity Assist (DVEGA) to JGA/Uranus. The JGA trajectory was chosen for its optimal blend of required launch energy and mission duration. Various Uranian moon-KBO combinations were evaluated against time-of-flight (TOF) for the JGA transfer, with the Ariel-G!kún‖'hòmdímà option proving the most ideal with a total baseline mission duration of 18 years, including a year of data downlink. Additional target combinations and launch opportunities are provided in the mission design section of this report.

Several launch vehicles are capable of providing the requisite launch energy of C3 = 121 m^2/s^2 for the mission, which was significantly less than the C3 = 161 m^2/s^2 for New Horizons, though none are currently listed as options in the PMCS guidelines. The Falcon Heavy Expendable launch vehicle with a Star 48BV upper stage was chosen for this concept and provides additional lift capability that can be allocated towards a larger propellant tank, thereby further increasing extended mission capability. Future science and system trades include investigating opportunistic science observations during each encounter, optimizing the use of the spacecraft's Ka-band performance to reduce the science downlink duration, and supporting the extended mission by enhancing propulsion capabilities (larger tank, additional thrusters) and evaluating mass and cost margins.

The inclusion of an additional imaging camera to supplement regional mapping during each close approach encounter can also be evaluated.

3. Technical Overview

3.1 Instrument Payload Description

The Calypso concept design consists of a total of ten science instruments placed on the spacecraft (nine unique), many of which were baselined from the New Horizons mission. Three imaging payloads, a radio science experiment, and a dust counter are direct holdovers from that proven design, while the remaining instruments, which consist of a pair of magnetometers and several instruments dedicated to measuring energetic particles (plasma, solar wind) were selected from recently completed missions or those currently in development. The cameras, magnetometer, radio science experiment, and at least one of the two plasma instruments are required to meet the threshold science objectives.

	Mass			EOL Peak Power		
	CBE (kg)	% Cont.[A]	MEV (kg)	CBE (W)	% Cont.[B]	MEV (W)
Vector Magnetometer (MAG) x2	6.63	24	8.21	4.20	20	5.04
Narrow Angle Camera (NAC)	11.14	20	13.37	5.50	20	6.60
Vis/NIR Imaging Spectrometer (Vis/NIR)	10.67	25	13.34	7.10	25	8.88
Radio Science Experiment (RS)	0.16	15	0.18	2.10	15	2.42
Ultraviolet Imaging Spectrometer (UVIS)	4.50	15	5.18	3.90	10	4.29
Ion Electrostatic Analyzer (I-ESA)	3.30	15	3.80	2.60	15	2.99
Electron Electrostatic Analyzer (E-ESA)	2.50	15	2.88	2.00	15	2.30
Energetic Particle Detector (EPD)	2.20	20	2.64	2.20	15	2.53
Dust Counter (D-Count)	1.69	20	2.03	5.02	10	5.52
baseline science support structure: brackets	*2.03*	*25*	*2.54*	–	–	–
Total Payload Mass	**44.82**	**21**	**54.15**	**34.62**	**17**	**40.56**

Exhibit 3-1. *Payload Mass & Power Table.*

a. % Contingency based on TRL and APL institutional practice, with 30% total margin included per stage as defined in and required by PMCS Ground Rules.
b. Contingency based on PMCS Ground Rules.

Vector Magnetometer (MAG). Calypso employs a pair of 3-axis, ring-core fluxgate detectors affixed equidistantly to a deployable 4-m mast boom to measure for traces of magnetic induction, dynamo, and/or remanence during close approach at Ariel and G!kúnǁ'hòmdímà. The presence of an induced internal magnetic field at Ariel would provide strong supporting evidence of a subsurface hydrosphere, making the dual MESSENGER-heritage instruments a critical component to meeting the highest priority scientific objective of the mission [Anderson 2007]. We do not expect a G!kúnǁ'hòmdímà magnetic field but a contingency measurement will be made. The spacecraft's thrusters will not be used during this period of time to minimize noise in the measurements.

Characteristics	Value	Units
Size/Dimensions (+ Boom)	4	m
Mass W/O Contingency (CBE)	6.63	kg
Avg Payload Power w/o Contingency	4.2	W
Data Rate Avg	1	kbps

Exhibit 3-2. *Vector Magnetometer (MAG) Characteristics.*

Characteristics	Value	Units
Size/Dimensions	61 x 31.4 x 31.4	cm x cm x cm
Mass w/o Contingency (CBE)	11.14	kg
Avg Payload Power w/o Contingency	5.5	W
Data Volume/Image	12.58	Mbits
FOV	0.29	deg
IFOV	5	mrad

Exhibit 3-3. *Narrow Angle Camera (NAC) Characteristics.*

Narrow Angle Camera (NAC). The NAC is a narrow-angle panchromatic imaging telescope with an aperture of 20.8 cm providing a 0.29-deg field of view (FOV) [Cheng 2008]. The Long Range Reconnaissance Imager (LORRI) NAC flown on New Horizons was used to refine the spacecraft's trajectory on its approach to Pluto while providing the highest resolution imagery gathered on the dwarf planet to date. The camera was used similarly in its encounter with the KBO Arrokoth during the spacecraft's extended mission. Calypso will use its NAC in the same manner, collecting full disk images of Ariel and G!kúnǁ'hòmdímà as well as <300-m resolution imagery at close approach to support the study of geomorphic properties and processes in an effort to uncover evidence of past collisions and the existence of subsurface layers.

Visible/Near-Infrared Imaging Spectrometer (Vis/NIR). The Vis/NIR is a multispectral imager comprised of a single optical telescope that supports the focal planes of two sub-instruments, the Multispectral Visible Imaging Component (MVIC) which covers the visible spectrum and the Linear Etalon Imaging Spectral Array (LEISA) for the infrared band [Reuter 2008]. Calypso will employ the MVIC similarly to its role on New Horizons, where it was responsible for the highest-resolution color images of Pluto ever taken. At resolutions between 5 km/pixel and <300 m/pixel, the instrument will generate global maps during each encounter to facilitate the study of the surface topography, geological history, and any surface-subsurface exchanges. Meanwhile, LEISA will be used to map surface features in the near-infrared region (<1 km/pixel) and to collect surface temperature data. Vis/NIR is a "pushbroom" scanning imager that requires the spacecraft to slew at a precise rate when making observations.

Characteristics	Value	Units
Size/Dimensions	49.5 x 40.6 x 29.5	cm x cm x cm
Mass w/o Contingency (CBE)	10.67	kg
Avg Payload Power w/o Contingency	7.1	W
Data Volume/Observation (variable)	782 (near C/A)	Mbits
HFOV (MVIC, LEISA)	5.7, 0.89	deg
IFOV (MVIC, LEISA)	20, 61	mrad

Exhibit 3-4. *Visible/Near-Infrared Imaging Spectrometer (Vis/NIR) Characteristics.*

Ultraviolet Imaging Spectrometer (UVIS). Based on the New Horizons Alice instrument, UVIS is an ultraviolet (UV) imaging spectrometer whose primary function is in the detection and/or observation of atmospherics [Stern 2008]. While neither Ariel nor G!kúnǁ'hòmdímà is expected to have an atmosphere, UVIS will contribute to the mapping of surface ices and mineral maps and will collect approach and look-back albedo images following each encounter.

Characteristics	Value	Units
Size/Dimensions	20 x 41 x 12	cm x cm x cm
Mass w/o Contingency (CBE)	4.5	kg
Avg Payload Power w/o Contingency	3.9	W
Data Volume/Observation (variable)	2–5	Mbits
FOV	2 (Airglow: 0.4x0.1)	deg
IFOV	0.3	mrad

Exhibit 3-5. *Ultraviolet Imaging Spectrometer (UVIS) Characteristics.*

Radio Science Experiment (RS). The essential components of RS are APL's ultra-stable oscillators (USO) and a custom field programmable gate array (FPGA) within the onboard radio. The highly accurate USOs enable the measurement of an uplink radio science signal to detect small changes in velocity in the presence of a gravitational field. The use of an uplink signal, rather than 2-way ranging, reduces peak power requirements during a period of high demand during the flyby [Tyler 2008].. Gravity measurements will be conducted at the same time as the magnetometer measurements at close approach, requiring the HGA to be pointed towards Earth prior to inhibiting the thrusters.

Characteristics	Value	Units
Size/Dimensions	n/a	cm x cm x cm
Mass w/o Contingency (CBE)	0.1	kg
Avg Payload Power w/o Contingency	2.1	W
Data Rate Avg	78.125	kbps

Exhibit 3-6. *Radio Science (RS) Experiment Characteristics.*

Characteristics	Value	Units
Size/Dimensions	13 x 10.2 x 11	cm x cm x cm
Mass w/o Contingency (CBE)	2.2	kg
Avg Payload Power w/o Contingency	2	W
Data Rate Avg (Slow, Fast, Burst)	0.8, 2.5, 6.5	kbps

Exhibit 3-7. *Energetic Particle Detector (EPD) Characteristics.*

Characteristics	Value	Units
Size/Dimensions	24.4 x 45.7 x 45.7	cm x cm x cm
Mass w/o Contingency (CBE)	3.3	kg
Avg Payload Power w/o Contingency	2.6	W
Data Rate Avg (Slow, Fast, Burst)	0.16, 0.5, 1	kbps

Exhibit 3-8. *Ion Electrostatic Analyzer (I-ESA) Characteristics.*

Energetic Particle Detector (EPD). EPD is a high-energy charged particle detector and a heritage instrument from the Magnetospheric Multiscale (MMS) observatory mission launched in 2015 [Mauk 2016]. The instrument is a modernized version of the energetic particle spectrometer (PEPSSI) flown on New Horizons [McNutt 2008]

Ion Electrostatic Analyzer (I-ESA). To measure solar wind particles and interstellar pickup ions (PUIs) along the spacecraft's path through the solar system, Calypso will use a simplified version of the Solar Winds Around Pluto (SWAP) instrument [McComas 2008] that is currently being developed for the Interstellar Mapping and Acceleration Probe (IMAP) mission launching in 2024. IMAP's Solar Wind and Pickup Ions (SWAPI) instrument removes its predecessor's retarding potential analyzer to increase transmission and improve detection sensitivity, providing scientists with more data to gain a better understanding of the distributions and properties of solar wind particles.

Electron Electrostatic Analyzer (E-ESA). The Solar Probe Analyzer B (SPAN-B) is a low-energy electron-focused detector hosted on the Parker Solar Probe currently conducting heliophysics observations in a highly elliptical orbit around the sun [Kasper 2016]. Coupled with the I-ESA and EPD instruments, E-ESA will be used to study the effects of Uranian magnetospheric plasmas on Ariel, as well as solar wind impingement on the surface of G!kún‖'hòmdímà and its moon.

Characteristics	Value	Units
Size/Dimensions	19.3 x 15 x 23.6	cm x cm x cm
Mass w/o Contingency (CBE)	2.5	kg
Avg Payload Power w/o Contingency	2	W
Data Rate Avg (Slow, Fast, Burst)	0.4, 0.8, 1.5	kbps

Exhibit 3-9. *Electron Electrostatic Analyzer (E-ESA) Characteristics.*

Characteristics	Value	Units
Size/Dimensions	45.7 x 30.5	cm x cm
Mass w/o Contingency (CBE)	1.69	kg
Avg Payload Power w/o Contingency	6.4	W
Data Rate Avg	10	bps

Exhibit 3-10. *Dust Counter (D-Count) Characteristics.*

Dust Counter (D-Count). The decision to include an instrument capable of detecting traces of microscopic dust on a mission to the outer solar system is an opportunistic one. The Student Dust Counter (SDC) flown on New Horizons carries negligible mass and data rates, but can be useful in researching regions of space for signs of past collisions or debris [Horányi 2008]. The latter case was determined to be one of the key findings in returned scientific data from the New Horizons mission where, during the approach to Pluto, there were concerns about hazardous debris ahead of the flyby. The SDC instrument was able to verify low detection rates of dust particles in the days leading up to the encounter, suggesting New Horizons would have safe passage through the region [Lauer 2019]. With a secondary encounter planned for the dwarf planet G!kún‖'hòmdímà and a mission that will likely extend further into the Kuiper Belt, Calypso's inclusion of this capability will be equally beneficial.

3.2 Flight System

Calypso's flight system is based heavily on the simple, reliable, cost-efficient, and proven heritage design of the New Horizons spacecraft [Fountain 2008]. Notable divergences from New Horizons will be called out in the subsystem sections below along with supporting reasons that led to any redesigns. A summary of the flight system is provided in Ex. 3-11 through 3-14; power details are provided in Appendix B.

	CBE (kg)	% Cont.	MEV (kg)
Propulsion	24.3	16%	28.1
Mechanical	192.1	15%	221.7
Thermal	27.6	10%	30.4
Power	91.7	7%	97.9
Guidance & Control	18.4	11%	20.4
Avionics (IEM)	19.7	15%	22.6
Telecommunications	63.0	12%	70.5
Harness	27.2	15%	31.3
Science Instruments	44.8	21%	54.1
Total Payload Mass	**508.6**	**13%**	**577.1**

Exhibit 3-11. *Flight System Mass Summary.*

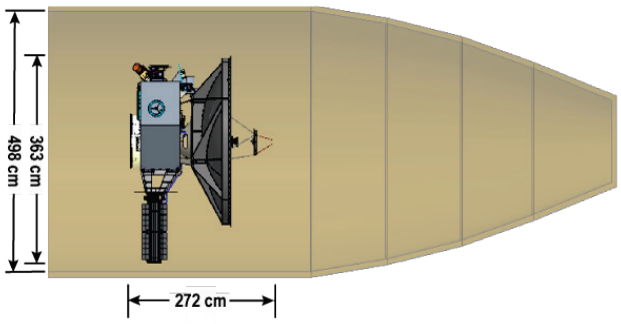

Exhibit 3-12. *Calypso in stowed configuration within a 5-m fairing, with clearances.*

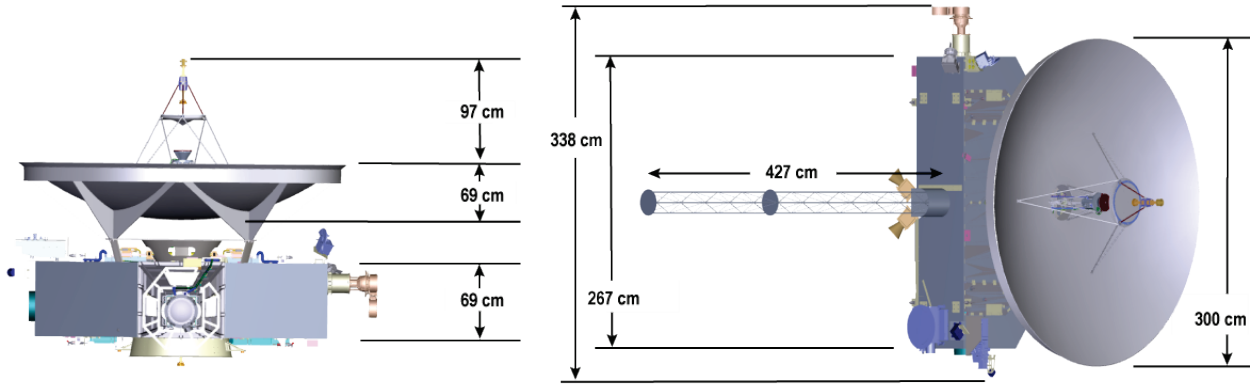

Exhibit 3-13. *Key Flight System Dimensions.*

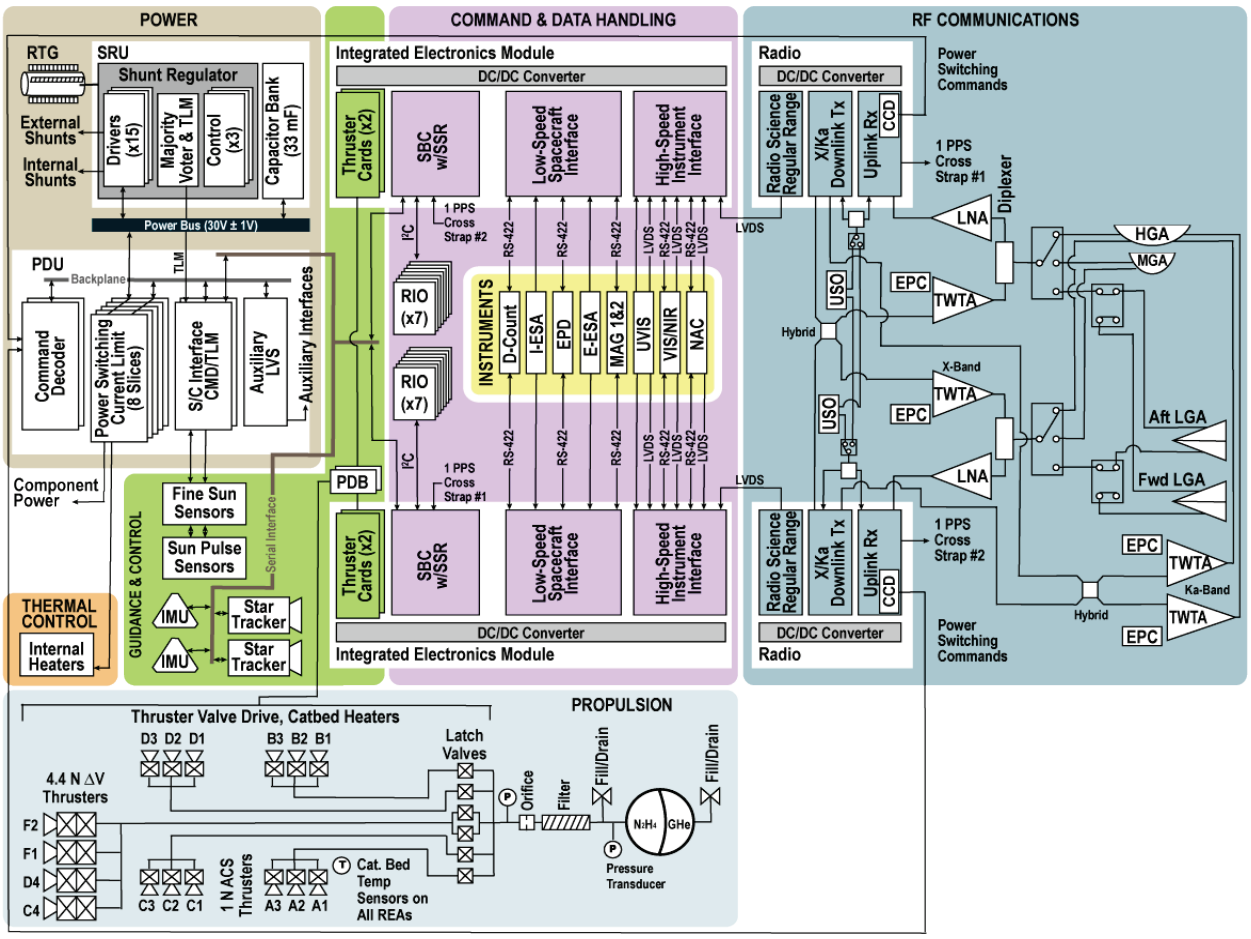

Exhibit 3-14. *Flight System Block Diagram.*

Propulsion. Calypso will use a blowdown monopropellant hydrazine system made up of 12 Aerojet Rocketdyne MR-103H thrusters for attitude control and 4 MR-111G thrusters for larger orbit correction and trim maneuvers, providing 1 N (0.2 lbf) and 4.4 N (1.0 lbf) of thrust, respectively. The spacecraft will use a 107 kg-capacity NGIS 80505 diaphragm tank flown on the Mars Science Laboratory (MSL) mission, taking advantage of the additional lift capacity delivered by the Falcon Heavy Extended launch vehicle. The tank is larger than the one enlisted by New Horizons, offering 19% more fuel capacity to be used in service of contingency operations and the extended mission (notably, only 77-kg of New Horizons' 90-kg tank was filled at launch as a result of the spacecraft's final dry mass and the maximum load capacity of the Atlas V 551) [Fountain 2008]. Considerations towards plume interference to sensitive instruments and propulsion system redundancy were made in the placement of each rocket engine assembly on the spacecraft. All four ΔV thrusters are pointed towards the –Y axis opposite the HGA, while the attitude control system (ACS) thrusters are distributed in each direction in the plane normal to the HGA and are fired in pairs to minimize residual ΔV. To reduce peak power requirements, the ACS is constrained to operate no more than two thrusters at a time for attitude control. During ΔV maneuvers, two additional thrusters may be operated simultaneously. The catalyst bed (catbed) heater wiring for ACS thrusters A1, A2, A3, B1, B2, and B3 will be combined to reduce switch requirements. Thruster cycle estimates are comparable to New Horizons, with <50% of the qualification limit (409,000 cycles) used for the Ariel encounter and <75% for the G!kún‖'hòmdímà flyby. A future trade for additional ACS thrusters is recommended to extend mission design life and extended mission capability.

Mechanical. The spacecraft's base structure is similar to New Horizons and is comprised of aluminum honeycomb paneling with a central support cylinder that houses the propellant tank. The structure has been widened to provide clearer fields of view for the instruments secured to the exterior panels in the presence of the larger 3.1-m HGA. The housing for the 4-m open-lattice magnetometer boom is located opposite the RTG along the X-axis. The placement of the boom, coupled with the use of three spin-balance mechanisms, will allow for realignment of the spacecraft's spin axis following deployment, which is expected to be on the order of ±0.25°

correction. To avoid obstruction by the extended boom, the three optical apertures of the NAC, Vis/NIR, and UVIS have been have been positioned on the +Z face of the structure. The star tracker apertures have been canted in the –Y direction, carried over from the New Horizons configuration. Calypso fits within a 5-m fairing in its launch configuration, with a minimum clearance of 16.5 cm between the RTG edge and the fairing shell.

Thermal. Calypso's design employs the same approach used by New Horizons, preserving a tightly coupled thermal environment for the internal components of the spacecraft. The core spacecraft temperature maintains a range of 5–50°C through the use of multi-layer insulation (MLI) wrapped around standoff clips bonded to the spacecraft decks, which also protects against micrometeoroid impacts. Mechanical restraints will be used around critical apertures and cutouts. The MLI and natural heat escaping from internal components comprise the majority of system heat loss, which is countered to a degree by electrical dissipation as well as some heat waste from the RTG [Fountain 2008]. The spacecraft leverages an autonomous, software-controlled heater system to balance bus temperatures with the thermal effects of dissipation during flight. The power distribution unit (PDU) distributes heat to an area on either the A or B side of the spacecraft via a string of heaters with power levels ranging from 2.5–30 W. The two sets of heaters are redundant backups to one another, with a dedicated system for the propulsion subsystem. There are four 7-blade thermal control louvers that help manage Calypso's heat rejection rates during early operations near Earth (maximizes heat rejection) and beyond Mars (minimizes heat rejection). Four external 10-W shunt elements can be switched internal later in the mission for additional heating inside the spacecraft.

Power. A single Next Generation General Purpose Heat Source Radioisotope Thermoelectric Generator (RTG) is required to power the spacecraft over the course of its mission to the outer solar system. A 56-kg Next Gen Mod 0 RTG, expected to be available by 2026, was selected for this concept design, providing 293 W of power at beginning of life (BOL) at a maximum average annual power degradation of 1.9% per year over an 18-year design life. Calypso's power is budgeted across all modes against a 30% margin tagged on to the estimated provision of the RTG over the lifetime of the spacecraft. If lower margins were permitted, the primary Calypso mission could be accomplished with any of the Next Gen RTGs (Mod 1 or later). The spacecraft bus voltage is maintained by the internally redundant shunt regulator unit with a large capacitor bank for transients. In addition, the power budget allocates 15 W for turn on transients and other scheduled events, such as latch valves and antenna switches. The PDU features internal redundancies, critical hold-off circuits, and a low voltage sense load shed. As with New Horizons, there is no battery for storing energy onboard the spacecraft.

Guidance & Control. Calypso operates in two distinct attitude control modes during the mission: Spin-Stabilized and 3-Axis. While in passive or active Spin-Stabilized mode, the spacecraft maintains a constant spin about its Y-axis at a rate of 2.5 rotations per minute (RPM), keeping its HGA fixed along this axis for telecommunications. The spin rate, which is half of the New Horizons spin rate of 5 RPM, was chosen to save propellant for the transitions between modes. Active Spin mode is employed while conducting normal operations, line-of-sight downlinks, during precessions, or when the spacecraft is attempting Earth or Sun Acquisition while in Safe mode. Passive Spin mode is used while the spacecraft is in hibernation during its cruise phase and in normal operations when not requiring attitude adjustments. The spacecraft transitions to a 3-Axis Stabilized mode while supporting science observations during each encounter. The NAC camera, which collects both staring and mosaic images, requires precise pointing at long ranges, while the Vis/NIR instrument operates entirely in a pushbroom scanning mode. Mass adjustment mechanisms are used to rebalance the spacecraft following magnetometer boom deployment to maintain HGA pointing while in a spin-stabilized attitude.

Calypso leverages a combination of redundant navigation instruments to provide accurate position and attitude information of the spacecraft. A pair of Leonardo AA-STR star trackers are mounted orthogonally below the magnetometer boom housing unit and provide 6 arc second accuracy to their boresights and 50 arc second accuracy about the boresight (3δ). Calypso utilizes a Honeywell Miniature Inertial Measurement Unit (MIMU) to measure accelerations and rotation rates about its three principle axes, which in turn are used to provide precise position, velocity and attitude data. With a mass of less than 5 kg, a second MIMU is included as a backup, but is not powered on unless required. Two New Horizons-heritage sun sensors manufactured by Adcole Space, one sun pulse sensor (SPS) and one fine sun sensor (FSS), work in conjunction to provide additional position information of Calypso relative to the sun [Fountain 2008]. When priority for the spacecraft's attitude is given to science observations, Calypso is capable of relying solely on its star trackers for attitude knowledge, albeit at a lower fidelity than when coupled with the IMU. All components were chosen for the purpose of establishing the baseline subsystem design. The selection of the actual components will go through the standard competitive procurement process for commercial-off-the-shelf (COTS) flight hardware several years prior to launch.

The aforementioned hydrazine ACS thrusters provide attitude control for the spacecraft during the mission lifetime while the more powerful ΔV thrusters support trajectory correction maneuvers (TCM). The ACS thrusters have three pulsing options spanning from minimum impulse bit (5 ms) to one minor frame (40 ms), which can also be used for continuous thrusting. The ΔV thrusters can be used while the spacecraft is operating in either attitude control mode. Passive Spin mode TCMs are finite maneuvers commanded from mission operations (open-loop) that are precisely timed and conducted along the spin axis only. Closed-loop Active Spin mode TCMs can incorporate the use of proportional thrusting from the ACS thrusters in the radial direction. When flying in 3-Axis mode, TCMs are able to use up to four thrusters simultaneously (2 ACS + 2 ΔV or 4 ACS) to conduct maneuvers in both axial and radial directions.

Avionics. The avionics subsystem tasked with managing the spacecraft's command and data handling requirements is based on designs used on both the Parker Solar Probe (PSP) and Europa Clipper missions. The single Integrated Electronics Module (IEM) leverages a slice-based architecture similar to the system used by PSP, with a multiplexer (MUX) joining the A and B sides for redundancy cross-strapping. Two single board computers (SBC) each provide 256MB of SDRAM, 8MB of MRAM (code storage), and 64Gb of flash memory with a UT700 100MHz processor. Additional PSP heritage-based components include a pair of Spacecraft Interface Cards (SCIF), four Thruster/Actuator Cards (TAC), two Instrument Interface Cards (IIF) with Solid State Recorders (SSR), and two DC/DC converters. Two strings of Remote Interface Units (RIUs) provide a total of 224 analog channels for temperature sensing. Four Propulsion Diode Boxes (PDB) planned for the Europa Clipper mission are used to mitigate electromagnetic interference effects caused during thruster firings. The IEM provides the capability to disable individual card when their functions are not needed to allow power to be used elsewhere. The ability to disable the TAC and IIF cards is necessary to achieve the dual-TWTA downlink capability while in a passive spinning mode.

Flight Software. Calypso uses onboard software to interpret uplinked commands and interface with various subsystems and related components while in flight. Guidance and control software supports the Spin-stabilized and 3-Axis attitude control modes previously described while providing precise pointing instructions to the science instruments during staring and scanning collections. It also directs control of the spacecraft's 16 thrusters, enabling the ability to conduct coupled or decoupled thruster firings as well as constrained (two ACS or two ΔV thrusters at once) or inhibited thruster operation. Command and data handling software handles all event-based (autonomous), time-tagged and macro commands provided to the system while managing the solid state recorder (SSR) functions, instrument data compression, memory scrubs, housekeeping data collection, and the data summary table. C&DH software is also responsible for the control of the heater system used to autonomously balance and maintain specific temperatures within the spacecraft bus. Testbed software will be used during ground operations to emulate system performance in various states during development, testing and integration.

Telecommunications. Calypso's tracking, telemetry, and control (TT&C) subsystem is comprised of a 3.1-m HGA, the APL Frontier Radio telecommunications system, and a 12-W traveling-wave tube amplifier (TWTA) that supports dual-TWTA downlinks with the Deep Space Network (DSN). The HGA assembly employs high, medium- and low-gain antennas centered on the parabolic reflector dish. A second low gain antenna is attached to the central support cylinder on the opposite side of the HGA to facilitate omnidirectional communications coverage during the launch and early operations phase (LEOP). This antenna is attached to the central support cylinder between the fuel tank and the launch vehicle payload adapter ring.

APL's Frontier Radio, which has flown successfully on the twin Van Allen Probe spacecraft, New Horizons, Parker Solar Probe, and most recently on the "Hope" Emirate Mars Mission, uses software to fine-tune the radio against specific mission requirements while using less power than many traditional spacecraft systems [Buckley 2021]. The system will also be used on upcoming missions including the Double Asteroid Redirection Test (DART), Europa Clipper, IMAP and Mars Dragonfly missions. Calypso will also include the ability to downlink at over 3× the baseline rate via Ka-band, though the precise pointing of ±0.06° required to maintain a link at this frequency may not be possible during all phases of the mission (specifically when the spacecraft is in Hibernation mode or is operating with thrusters inhibited during close approach). Therefore, all communication requirements are met with the dual TWTA X-band downlink and pointing accuracy of ±0.2°.

The design of the telecommunications subsystem is based in part on the availability of the DSN of ground station antennas traditionally used to support long-range unmanned space missions. Guidelines provided by this decadal mission concept study dictate that the use of the 70-m antennas is minimized or otherwise avoided altogether. As a result, the Calypso baseline mission is specifically designed with the capabilities provided by

the 34-m DSN antennas in mind, leading to the selection of the 3.1-m HGA, roughly 1-m larger in diameter than that used during the New Horizons mission which did have the benefit of the larger ground antennas.

Four arrayed 34-m DSN antennas will be required to support the high data volume rates expected during the encounter phases in the days surrounding each flyby, approximately 10 days before and 4 days after each event. An additional year of downlink time is allocated for science data following each encounter. In total, 23.7 Gbits of data are estimated to be collected during the Ariel flyby, while an additional 3.9 Gbits are expected at G!kúnǁ'hòmdímà. A total of 17,871 hrs of DSN coverage using the 34-m dishes is expected to accommodate these data volume estimates across 2,488 passes.

Radiation. Radiation exposure for Calypso consists of both natural and RTG-induced sources. The total dose radiation requirement is 30 krad for the baseline Calypso mission. This includes radiation design margins (RDMs) of 2 for the solar proton, Jupiter, and Uranus environment contributions, and 1.5 for the RTG contribution. The solar proton environment is specified at the 95% confidence level.

Calypso will be launched directly into its trajectory to Jupiter, minimizing the amount of exposure it will have to Earth's Van Allen belts of trapped energetic particles. Total ionizing dose (TID) accumulation during launch ascent is estimated at <1 krad. The trajectory also minimizes time in the inner solar system during cruise, where the predicted contribution from solar protons is 5 krad based on the ESP-PSYCHIC model, which scaled as 1/r outbound from the Sun at a 95% confidence level. The radiation environment contribution from the Jupiter flyby at 24 Jovian radii (Rj) is predicted to be 1 krad contribution using the GIRE3/Grid3p model, which leverages more accurate data than what was available while planning for the New Horizons' 2007 JGA. The JPL Uranian Model (UMOD) leverages measurement data collected on the Voyager 2 probe flyby in 1986 and is the only model available to provide insight into the radiation environment of the Uranian system. Referencing this model, Calypso is expected to encounter mainly trapped electrons during its flyby of Ariel with an estimated dose of ~200 rad at a distance of 4 Uranian radii [Garrett et al. 2015]. The radiation environment during the flyby of G!kúnǁ'hòmdímà, along with the extended mission to a Kuiper Belt object, is considered negligible.

For the RTG contribution, we considered gamma and other particle radiation. As with Cassini and New Horizons, the total dose from the RTG gamma ray spectrum was calculated using a radiation dosage monitor (RDM) of 1.5. The nominal shielding we have adopted to derive the total dose hardness requirement is 0.5 g/cm^2. A detailed, three-dimensional shielding analysis of the spacecraft, including variations in shield depth and material density, is planned for later in mission development. For this three dimensional analysis, experimental measurements of the RTG neutron and gamma flux would be included as inputs to the modeling.

The RTG also introduces a neutron background to the spacecraft, centered at a neutron energy of about 2.5 MeV. An 18-year mission will result in an exposure of no more than 3x10^{10} n0/cm^2 (including an RDM of 1.5 over the predicted fluence of 2×10^{10} n0/cm^2) even in the absence of shielding to an electronics unit at a distance of 2 m from the RTG. The primary potential damage these neutrons can produce is damage to optical sensors and electro-optic components, owing to solid-state displacement damage effects. Instrument placement on the opposite side of the spacecraft from the RTG, minimizes the radiation contribution from the RTG. As required localized spot shielding of electronic parts is planned.

Components selected for this concept design meet the 30 krad part-hardness requirement. Additional radiation effects including total non-ionizing dose (e.g., displacement damage) and single-event effects (SEE) are in-family with those of New Horizons, while the detector noise and charging while operating in the Uranian system assumes similar levels to that encountered in Earth orbit.

3.3 Mission Design & Concept of Operations

3.3.1 Mission Design Overview

The central theme of the Calypso mission design is flexibility. The mission design analysis identified multiple trajectory options spanning multiple launch years, meeting the scientific requirement of ocean world flybys of an ice giant moon and a dwarf planet KBO, providing the capability for an extended mission flyby of an additional KBO, and fitting within a launch vehicle performance comparable to the New Horizons mission. The results of the analysis are listed in Ex. 3-19, 3-20, and 3-21, while the analysis process and baseline trajectory are described in detail in this section.

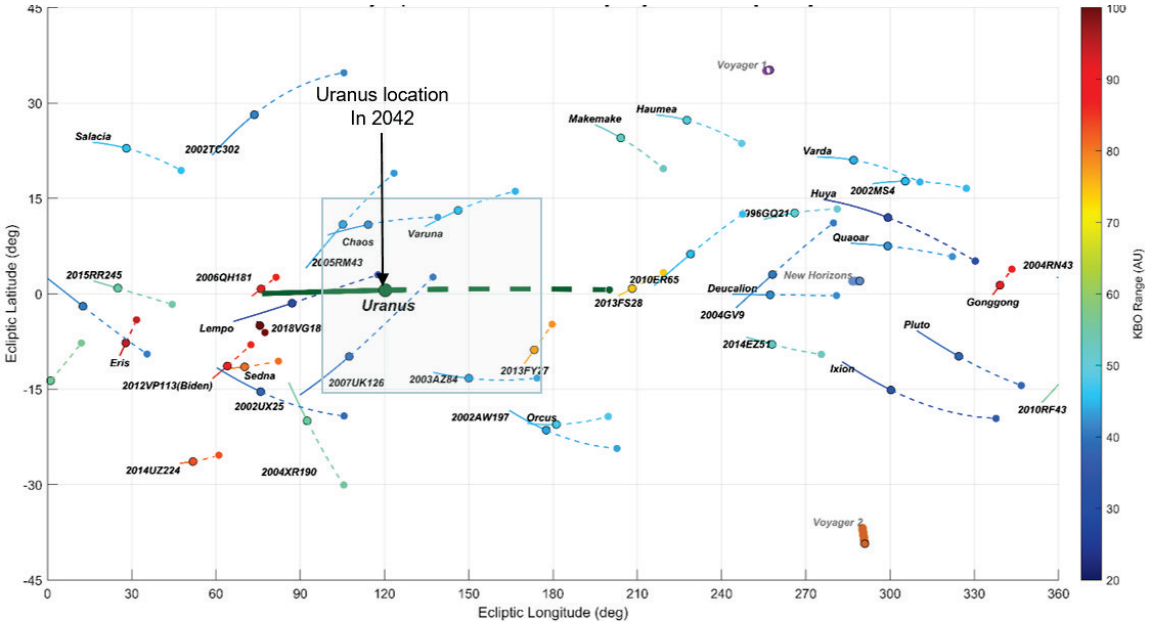

Exhibit 3-15. Sky Map for KBOs. *For each object depicted in the sky map, the solid line plots the location of the object in the sky from 2030–2042. The circular marker corresponds to the location in 2042 followed by the dashed line plotting the location from 2042–2057. The highlighted box indicates the estimated accessibility enabled by the Uranus gravity assist. As Uranus moves in its orbit from left to right, the accessibility box, and thus the accessible dwarf planets, is a function of where in the sky Uranus is at the time of the encounter.*

Uranus was chosen as the primary ice giant system for the baseline design of the Calypso mission, consisting of encounters with either of the planet's moons Miranda or Ariel to satisfy scientific requirements. Several transfer options were considered to reach the Uranian system: Direct-to-Uranus, a Jupiter Gravity Assist (JGA) en route to Uranus, and a 3-year ΔV Earth Gravity Assist (DV-EGA) followed by a JGA en route to Uranus. Although annual launch opportunities can be accommodated by the Calypso mission constraints, the JGA to Uranus was selected for the baseline concept design due to reduced launch energy and shorter mission duration. The JGA provides the opportunity for Calypso to carry more propellant, further enhancing the capability for an extended mission flyby of an additional KBO.

Transfer Sequence Construction. Accessible KBOs after the Uranian system encounter are determined by their proximity to Uranus as projected in the ecliptic sky. From a broad search of transfer trajectories, it was determined that the optimal launch timeframe for the JGA to Uranus transfer occurs between 2033–2035, with the Uranian system encounter approximately 6–7 years later. Based on this timing, the ecliptic sky map shown in Ex. 3-15 was constructed to chart which potential dwarf planets were in the accessible part of the sky following a Uranus flyby in 2042. For the purposes of Calypso, we assumed KBOs with diameters ≥ 600 km were most likely dwarf planets based on the most conservative estimates from Lineweaver and Norman [2010].

For the trajectory options with a Uranian system arrival in the 2042 timeframe, the reachable KBOs larger than 600 km were Chaos, Varuna, 2003 AZ84, and G!kún‖'hòmdímà. For each of these KBOs, the intercept point of the Uranian moon plane was analytically reconstructed from the broad search results to approximate the transfer time for a given Uranian moon/KBO pair (Ex. 3-16). Examining the results in Ex. 3-16, two main

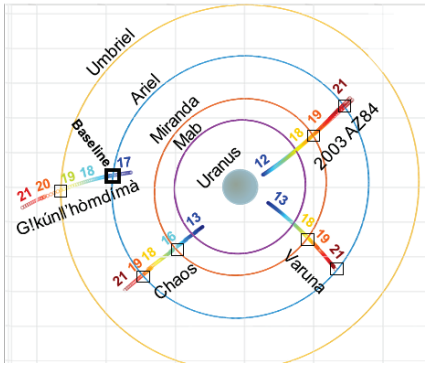

Exhibit 3-16. Uranian Moon Plane Crossing Points for Earth-Jupiter-Uranus-Varuna broad search results. *Each square marker represents a Uranian moon/KBO flyby combination identified from a broad search 1000's of flyby trajectories. The rainbow colored plots show the transfer time in years from launch to the KBO encounter. The baseline Ariel/G!kún‖'hòmdímà combination was selected as the shorted flight duration involving an Ariel flyby.*

design constraints were understood: (1) the fastest flight time solutions were only possible with close passage of Uranus (ruling out the more distant Uranian moons) and (2) a flyby of Miranda will always have a shorter total mission duration, as compared to a flyby of Ariel to the same KBO. Regardless, a slight preference was given to the Ariel flyby, and the Ariel/G!kúnǁ'hòmdímà combination was selected as the baseline trajectory.

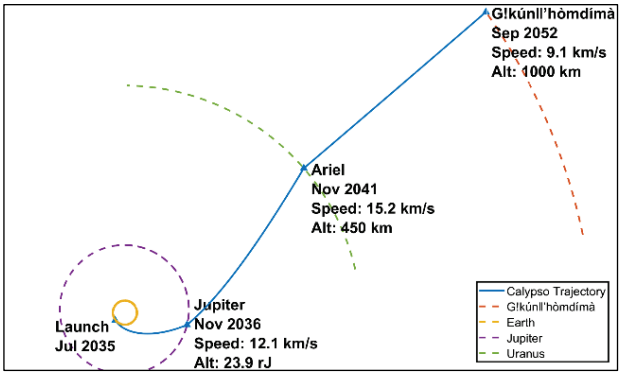

Exhibit 3-17. *Calypso baseline trajectory with launch in 2035.*

Baseline Trajectory. The baseline Ariel/G!kúnǁ'hòmdímà trajectory for Calypso is shown in Ex. 3-17. There are 21 launch opportunities that span the period between 11–31 Jul 2035 with a maximum TOF of 17.1 years from launch to G!kúnǁ'hòmdímà and a maximum launch energy of 121 km^2/s^2. While the trajectory has zero deterministic ΔV, the Calypso spacecraft has the ΔV capability to accommodate navigation uncertainties for all planned encounters, including a 450 km altitude flyby of Ariel, as well as unallocated margin that can be potentially used for an additional KBO flyby extended mission. The full spacecraft ΔV budget can be found in (§ 3.2). Geometric details of major trajectory events can be found in Ex. 3-18.

Event Date	Body	Encounter Alt.(km)	V-infinity (km/s)	Solar Phase Ang. (deg)	Earth Ang. (deg)	SEP (deg)	SPE (deg)	Sun Range (AU)	Earth Range (AU)
2035 Jul 11	Launch		10.87						
2036 Nov 16	Jupiter	1708274.76	12.09	25.89	31.30	150.93	5.42	5.08	4.20
2041 Nov 01	Uranus	144938.86	12.39	12.32	15.39	86.45	3.07	18.50	18.53
2041 Nov 01	Ariel	450.00	15.24	32.42	34.66	86.52	3.07	18.50	18.53
2052 Sep 09	G!kúnǁ'hòmdímà	1000.00	9.09	39.97	40.79	36.37	0.90	37.83	38.63
2061 Jan 09	End of Kuiper Belt							50.00	

Exhibit 3-18. *Calypso Mission Milestone Events Data.*

Launch Vehicle Compatibility. Although the baseline Calypso trajectory requires significantly less launch energy compared to New Horizons (121 km^2/s^2 vs. 164 km^2/s^2), its required launch capability exceeds the current PMCS ground rules that caps performance to a launch vehicle comparable to a Falcon Heavy Recoverable. Even so, there are feasible launch configurations, requiring an additional STAR48 kick stage (similar to New Horizons), that are expected to be available in the Calypso launch timeframe. Both the Falcon Heavy Expendable and Vulcan6, with a kick stage, can support the Calypso mission design with excess lift capability, which could be used to accommodate a larger propellant tank and increase the KBO extended mission capability beyond those described in this report.

Alternate Launch Opportunities. As stated previously, although the 2035 Ariel/G!kúnǁ'hòmdímà trajectory was selected as the baseline, several other candidate dwarf planet solutions with flybys of either Ariel or Miranda are possible within the Calypso mission requirements. Examples of alternate launch opportunities are included in Ex. 3-19, demonstrating the flexibility that can be accommodated by the Calypso mission.

Launch Year	Launch Date	Jupiter Encounter	Ocean World Encounter	Dwarf Planet Encounter	Ocean World	Dwarf Planet	C3 (km^2/s^2)	Time of Flight (years)
2035	**Jul 2035**	**Nov 2036**	**Nov 2041**	**Sep 2052**	**Ariel**	**G!kúnǁ'hòmdímà**	**121**	**17.1**
2034	Jul 2034	Feb 2036	Oct 2041	Sep 2053	Ariel	G!kúnǁ'hòmdímà	120	19.2
2034	Jul 2034	Jan 2036	Feb 2041	Aug 2051	Miranda	Chaos	120	17.1
2034	Jul 2034	Mar 2036	Jul 2042	Jul 2055	Ariel	Varuna	135	21.0
2034	Jul 2034	Feb 2036	Aug 2041	Jan 2052	Miranda	Varuna	135	17.5
2035	Jul 2035	Nov 2036	May 2041	May 2051	Miranda	Chaos	120	15.8
2035	Aug 2035	Dec 2036	Feb 2042	Jan 2053	Miranda	Varuna	135	17.4
2035	Aug 2035	Dec 2036	Jan 2043	Nov 2056	Ariel	Varuna	135	21.3
2036	Sep 2036	Sep 2037	Apr 2042	Nov 2053	Ariel	Chaos	162	17.2
2036	Sep 2036	Oct 2037	Feb 2043	Apr 2055	Miranda	Varuna	150	18.6

Exhibit 3-19. Alternate Launch Opportunities*. Current baseline trajectory highlighted in first row.*

While not studied as extensively as the Uranus options, the Calypso design can accommodate Neptune launch opportunities with a flyby of Triton followed by a dwarf planet flyby. Some feasible Neptune transfers are identified in Ex. 3-20. Due to Jupiter-Neptune phasing, the optimal launch for JGA-to-Neptune occurs from 2031–2033. For Neptune options, the acceleration from JGA helps counteract the large Neptune flyby distance required to encounter Triton. With a more thorough examination of Neptune options and an expanded KBO target list, Neptune solutions with transfer times comparable to the Calypso baseline can be expected. A Triton/Eris trajectory has great scientific interest and is included in Ex. 3-20 to illustrate that the launch requirements would likely push it outside of a New Frontiers-class mission concept for the current decadal launch timeframe due to the large launch energy of 297 km^2/s^2.

Launch Year	Launch Date	Jupiter Encounter	Ocean World Encounter	Dwarf Planet Encounter	Ocean World	Dwarf Planet	C3 (km^2/s^2)	Time of Flight (years)
2028	Jun 2028	--	Sep 2034	Aug 2049	Triton	Eris	297*	21.2
2030	Feb 2030	Jun 2032	Aug 2046	Nov 2063	Triton	Salacia	154	33.7
2031	Jan 2031	Dec 2032	Sep 2043	Aug 2063	Triton	Sedna	135	32.5
2032	Mar 2032	Sep 2033	Aug 2044	Oct 2065	Triton	Sedna	131	33.6

Exhibit 3-20. Neptune/Triton Launch Opportunities. ** Eris trip exceeds design parameters.*

Direct-to-Uranus missions can be accommodated by Calypso and enable yearly launch opportunities. Compared to JGA trajectories in Ex. 3-19, direct solutions will require higher launch energy, but are still within the design limits of a New Frontiers-class mission concept, as the solutions are in family with New Horizons. A few example trajectories are shown in Ex. 3-21, validating nearly annual launch opportunities exist into the next decade, and can accomplish the Calypso science objectives of close encounters with an ocean world and dwarf planet. Solutions for the 2037–2040 launch years are feasible, but will require transfer times closer to 20 years or revisiting the limited target list.

Launch Year	Launch Date	Ocean World Encounter	Dwarf Planet Encounter	Ocean World	Dwarf Planet	C3 (km^2/s^2)	Time of Flight (years)
2030	Aug 2030	Jul 2036	Jan 2046	Miranda	Chaos	165	15.4
2030	Aug 2030	May 2037	Mar 2049	Ariel	Chaos	154	18.6
2031	Aug 2031	Dec 2037	Nov 2048	Ariel	Chaos	159	17.3
2032	Aug 2032	Jul 2038	Nov 2048	Ariel	Chaos	165	16.2
2040	Sep 2040	Sep 2046	May 2059	Ariel	Varuna	161	18.7
2041	Sep 2041	Jul 2047	Jan 2060	Ariel	Varuna	163	18.3
2042	Oct 2042	Jun 2048	Jun 2061	Ariel	Varuna	164	18.7
2041	Sep 2041	Feb 2048	Apr 2058	Ariel	2003 AZ84	154	16.5
2042	Oct 2042	Nov 2048	Oct 2058	Ariel	2003 AZ84	157	16.0
2043	Oct 2043	Oct 2049	Oct 2059	Ariel	2003 AZ84	158	16.0

Exhibit 3-21. Direct-to-Uranus Launch Opportunities.

Mission Design Summary. The Calypso mission design offers tremendous flexibility, providing wide-ranging trajectory options that meet the scientific requirements of ocean world flybys of an ice giant moon and a dwarf planet KBO while offering the capability for an extended mission to encounter an additional KBO. Though the baseline trajectory uses the opportunistic JGA to take advantage of lower launch energy and higher propellant stores, Direct-to-Uranus missions can also be accommodated by Calypso to enable nearly annual launch opportunities spanning more than a decade.

3.3.2 Mission Operations

Calypso's mission operations can support at least three flyby encounters, including an extended mission into the Kuiper Belt, using established APL Mission Operations Center (MOC) facilities and infrastructure. Personnel will monitor the spacecraft health and status during its mission lifetime, as well as manage flyby targeting operations. In preparation for each encounter, rigorous ground testing of instrument sequences on the operations simulator will be conducted, followed by selected inflight tests. A single end-to-end inflight rehearsal will occur prior to the first encounter. The concept leverages a coupled mission operations approach that combines instrument and spacecraft commanding into a single sequence. From a conceptual operations standpoint, this same strategy was used on New Horizons and is planned for use on NASA's Dragonfly mission to Titan. Uplinks will employ the CCSDS File Delivery Protocol (CFDP) while downlinks will be handled based on similar processes used during the MESSENGER mission.

Prior to the Uranian moon encounter, Calypso's data downlinks will predominantly consist of housekeeping, commanding, and system checkouts, with navigation observations, where needed, to adjust the spacecraft's trajectory, particularly around the JGA event. The spacecraft will mostly operate in a spin-stabilized Beacon Hibernation mode with annual checkout activities following the flyby of Jupiter and between encounters. Hibernation operations reduce the amount of fuel consumed and number of required DSN contacts during transit. While particle and plasma measurements will be recorded throughout the majority of the mission lifetime at an average combined data rate of 3.86 kbps across the EPD, E-ESA, I-ESA, and D-Count instruments, primary science collections will begin on the target bodies during the Approach Observatory Phases several months before each encounter. Observations will increase in frequency over time until reaching the period of the heaviest data collection during the Near Encounter Phase of each flyby.

A preliminary schedule of observations was developed against the collection parameters required by the science objectives to approximate the total data volume expected for the Near Encounter Phase of the flybys. Both the magnetometer and radio science experiments are expected to collect for 30 min centered on the point of closest approach during each encounter, with data collection rates of 1 kbps and 78.125 kbps, respectively. Each observation by the NAC is assumed to be a three-image burst collection, while mapping by the Vis/NIR is dependent on the specific scan rates of its components and the distance to each of the targets, which include the encountering bodies as well as other targets of opportunity presented with the baseline mission design (e.g., moons, ring systems). The total data volumes for each Near Encounter Phase includes 24 hours of plasma and particle instrument collection both before and after the closest approach. While observations by the lower priority UV spectrometer were not included in the creation of the notional collection schedule, additional studies to refine the collection plan would incorporate those accordingly. The post-Uranian moon encounter science data return is estimated to be 18.8 Gbits, for which we have allocated a subsequent DSN downlink data volume of 23.7 Gbits. The data volume collected during the subsequent encounter with the dwarf planet was calculated as 2.5 Gbits of data, for which we have allocated 3.9 Gbits of subsequent DSN downlink data volume.

As specified in the PMCS ground rules, a single 34-m DSN antenna shall be baselined to support nominal operations outside of any planned critical events, radio science experiments, or navigation observations. Additionally, the availability of a 70-m DSN antenna can be assumed during emergency situations. Calypso can achieve its expected downlink performance outside of encounter phase operations using one 34-m antenna, while the 70-m or equivalent (4 × 34m arrayed antennas) will be needed to support two weeks of continuous coverage 10 days prior and 4 days after each of the two encounters. Following each flyby event, the spacecraft will scale back to nominal operations coverage to support the science data returns estimated to continue up to one year following each encounter. In total, 17,871 hours of DSN coverage across 2,488 passes is needed to support the entire mission.

The PMCS ground rules also state that a baseline mission shall make use of Ka-Band downlinks for all science data returns, where possible, to support NASA's transition to this band for all future deep space missions. While the baseline design of the spacecraft includes the ability to transmit via Ka-Band, the precise pointing required for Ka-Band downlinks (± 0.06°) will not be possible during all phases of the mission. Extended periods of Ka-Band downlink while in a 3-Axis mode would prematurely exhaust the spacecraft resources. Based on this constraint, Calypso's downlink requirements, as defined by the estimated downlink data volume and available DSN coverage, are met by leveraging the spacecraft's dual X-Band TWTAs and HGA antenna. Whenever possible, the Ka-Band will be used to reduce the duration of the science downlink, however, the baseline mission operations plan does not require the use of Ka-band.

3.4 Risk List

The associated risks of the proposed baseline mission were assessed for both likelihood (L) and consequence (C) during this concept study. There are 7 notable risks outlined below, with their likelihood and consequence assessment rankings provided alongside their respective technical (T) or cost/schedule (S/C) classifications.

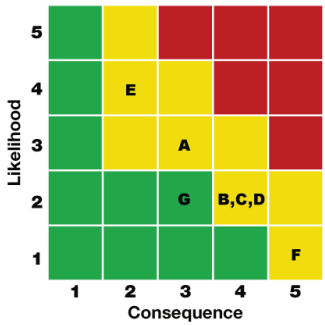

Exhibit 3-22. *Summary of Calypso risks. See table below for details.*

ID	Risk (Type, LxC Rating)	Mitigation
A	**Electrical Power Margin** IF the RPS has lower electrical power than currently rated, THEN insufficient power margin could exist. May adversely affect extended mission performance. (T, 3 x 3)	Flexible spacecraft operations concept to enable graceful degradation in the event of reduced power margins.
B	**Magnetic Cleanliness** IF spacecraft-generated magnetic fields are higher than expected, THEN magnetometer measurements may be degraded. Sensitivity for measurement of subsurface oceans may be affected. (T, 2 x 4)	Develop a strict magnetic cleanliness requirements and verification process.
C	**Launch Vehicle NEPA Approval** IF LV NEPA certification is delayed, THEN the launch may also be delayed. VULCAN, Falcon Heavy NR both need NEPA certification. (S/C, 2 x 4)	Similar to New Horizons, start development of data books early for both LV options. Select LV around project PDR, based on the most currently available launch manifest and historical performance.
D	**DSN Compatibility** IF 70m (or equivalent 4x34m) dish is not available, THEN the critical events coverage to downlink optical navigation data would impact targeting accuracy. (T, 2 x 4)	Perform detailed navigation assessment early in the project and work closely with DSN to ensure critical capabilities are maintained.
E	**Launch Vibration Loads** IF the chosen LV has vibration loads greater than the Atlas V, THEN additional analysis and structural mass may be needed. (T, 4 x 2)	Design system to the envelope of the environments of the available launch vehicle options. LV performance margin exists for additional mass, if necessary.
F	**Launch Vehicle Availability** IF a Falcon 9 Heavy Expendable with a STAR48 kick stage (or launch vehicle of equivalent capability) is not available, THEN the mission cannot be executed. (T, 1 x 5)	No project level mitigation is feasible. Heavy lift vehicle is required.
G	**Radiation** IF radiation analysis requires additional radiation hardness, THEN higher cost parts or additional shielding could be required. (T, 2 x 3)	Perform detailed 3-dimensional radiation modelling analysis early in the project. Robust mass margins and cost reserves could be applied to additional shielding and/or parts procurement costs.

Exhibit 3-23. *Calypso risks are well understood and easily managed.*

4. Development Schedule & Schedule Constraints

4.1 High-Level Mission Schedule

Calypso's high-level mission schedule (Ex. 4-1) is based on that developed for New Horizons and other missions of similar scope and complexity within the New Frontiers program. Mission-level gateway milestones (Ex. 4-2) and key phases and durations (Ex. 4-3) are included in the tables below.

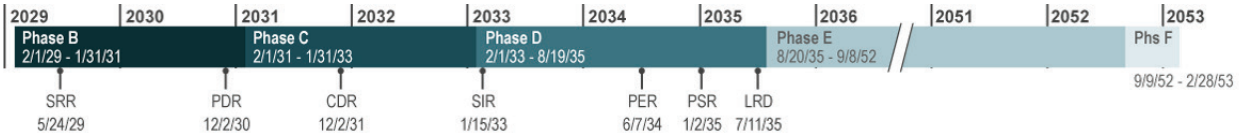

Exhibit 4-1. *High-Level Mission Schedule.*

Project Phase	Approximate Duration
Phase A – Conceptual Design	12 mo.
Phase B – Preliminary Design (excl. Phase B Bridge)	24 mo.
Phase C – Detailed Design	24 mo.
Phase D – Integration & Test	31 mo.
Phase E – Primary Mission Operations	207 mo.
Phase F – Extended Mission Operations	6 mo.
Start of Phase B to PDR	22 mo.
Start of Phase B to CDR	35 mo.
Start of Phase B to Delivery of First Instrument	52 mo.
Start of Phase B to Delivery of Last Instrument	57 mo.
Start of Phase B to Delivery of First S/C Bus Component	39 mo.
Start of Phase B to Delivery of Last S/C Bus Component	67 mo.
System Level Integration & Test	30 mo.
Project Total Funded Schedule Reserve	6 mo.
Total Development Time Phase B–D	80 mo.

Exhibit 4-1. *Key Mission Phase Durations.*

Mission Level Milestones	Date
System Requirements Review (SRR)	5/24/2029
Preliminary Design Review (PDR)	12/2/2030
Integrated Baseline Review (IBR)	7/15/2031
Critical Design Review (CDR)	12/2/2031
Mission/Science Operations Review (MOR/SOR)	3/31/2032
System Integration Review (SIR)	1/15/2033
Operational Readiness Review (ORR)	5/11/2033
Pre-Environmental Review (PER)	6/7/2034
Pre-Ship Review (PSR)	1/2/2035
Mission Readiness Review (MRR)	2/8/2035
Safety & Mission Success Review (SMSR)	3/16/2035
Launch Readiness Review (LRR)	7/2/2035
Launch Readiness Date (LRD)	7/11/2035

Exhibit 4-2. *Mission-Level Milestones.*

4.2 Technology Development Plan

The proposed baseline spacecraft design is comprised entirely of heritage-based technology flown on recent, current, or planned space missions. All components have a test readiness level of 6 or higher and will require no additional technology development or funding to increase their TRL levels before the proposed launch date.

4.3 Development Schedule & Constraints

The critical path for the Calypso mission involves the availability of a suitable power source (the Next Generation Mod 0 RTG selected for this study is expected in 2026) and the associated launch window for a chosen set of celestial body targets. Mission designs considered for this concept study are constrained by the suggested project start date in the PMCS ground rules spanning 2023–2032.

5. Mission Life Cycle Cost

5.1 Introduction

The cost estimate prepared for the Calypso mission is of concept maturity level (CML) 4. The payload and spacecraft estimates capture the resources required for a preferred point design and take into account subsystem level mass, power, and risk. Our estimate also takes into account the technical and performance characteristics of the components. Estimates for science, mission operations, and ground data system elements, whose costs are primarily determined by labor, take into account the Phase A–D schedule and anticipated Phase E timeline.

The Calypso Phase A–D mission cost, including unencumbered reserves of 50% and LV costs, is $1.1B in fiscal year 2025 dollars (FY$25), as shown in Ex. 5-1. Excluding all LV-related costs, the Calypso Phase A–D mission cost is $877M FY$25.

WBS		Ph A–D	Ph E–F	Total	Notes
1	Program Management	$67,444		$67,444	15.9% of payload, S/C, I&T (average of historical missions: VAP, PSP, NH). Wrap factor based on recent New Frontiers and APL missions. Phases E–F in WBS 7.
2	Systems Engineering				
3	Mission Assurance				
4	Science	$28,255	$110,398	$138,653	Cost per month of recent New Frontiers and APL missions.
5	Payload	$110,996		$110,996	Average of analogy and two parametric estimates.
6	Spacecraft (S/C)	$265,499		$265,499	Parametric estimate with propulsion ROM with RTG costs from Decadal guidelines.
7	Mission Operations (Mops)	$23,143	$407,463	$430,606	Cost per month average of NH, Osiris-Rex, and PSP plus DSN.
8	Launch Vehicle	$276,000		$276,000	Est ($210M for Falcon Heavy Expendable, $40M for upper stage) – plus $26M RTG surcharge.
9	Ground Data System	$24,021	$15,272	$39,293	Bottoms-up engineering estimate plus NH testbeds.
10	Integration & Test (I&T)	$47,680		$47,680	12.7% of payload and S/C (average of historicals).
	Total (w/o reserves and w/ LV)	**$843,037**	**$533,133**	**$1,376,171**	
	Total (w/o reserves and w/o LV)	**$567,037**	**$533,133**	**$1,100,171**	
	Reserves (50% A–D, 25% E–F)	**$283,519**	**$126,084**	**$409,603**	**Per Decadal guidelines**
	Total (w/reserves and w/LV)	**$1,152,556**	**$659,217**	**$1,811,773**	
	Total (w/reserves and w/o LV)	**$876,556**	**$659,217**	**$1,535,773**	**Assume $1.1B cost cap ($850M in FY15) excluding LV and RTG, including $26M surcharge.**

Exhibit 5-1. *Estimated Phases A–F Calypso mission cost (FY$25K) by Level-2 WBS element.*

5.2 Mission Ground Rules & Assumptions

- Estimating ground rules and assumptions are derived from the PMCS ground rules dated Feb 2021.
- Mission costs are reported using the Level-2 (and Level-3 where appropriate) work breakdown structure (WBS) provided in NPR 7120.5E.
- Cost estimates are reported in fiscal year 2025 (FY25) dollars.
- The NASA New Start inflation index provided by the PSMS Headquarters (PMCS HQ) was used to adjust historical cost, price data, and parametric results to FY25 dollars if necessary.
- The mission does not require technology development investment to advance components to TRL 6 because all Calypso mission components will be at or above TRL 6 when required.
- A launch vehicle of sufficient capability to support the Calypso mission is in development. Our assumption is that a launch vehicle meeting mission requirements will be available by 2030. Launch vehicle costs are estimated based on the expected capability.
- This estimate assumes no development delays and an on-time launch in Jul 2035.
- Phase A–D cost reserves are calculated as 50% of the estimated costs of all components excluding the launch vehicle. Phase E–F cost reserves are calculated as 25% of the estimated costs of all Phase E elements excluding DSN charges.

5.3 Cost Benchmarking

The cost and scope of the Calypso concept corresponds well to a NASA New Frontiers-class mission (see Ex. 5-2). The estimated cost to develop and operate Calypso compares favorably to New Frontiers missions currently under development, as well as to past New Frontiers missions, with an average cost of $1B, excluding launch vehicle costs.

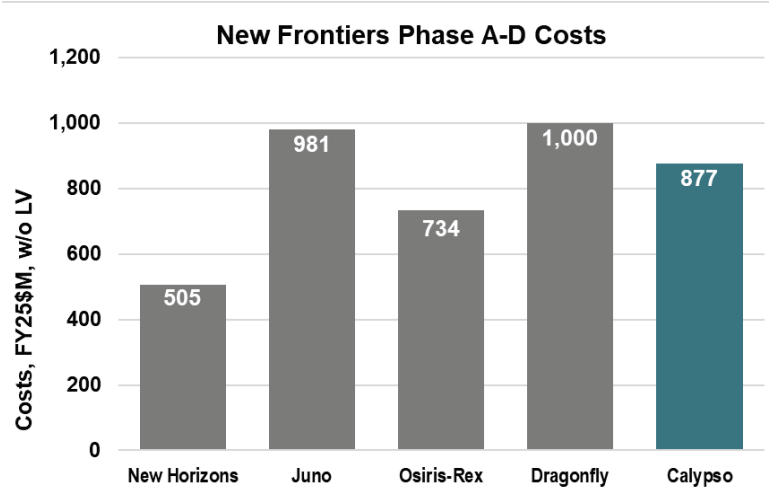

Exhibit 5-2. *Mission-level cost comparison (FY$25K) to other New Frontiers.*

5.4 Costing Methodology & Basis of Estimate

The Calypso CML 4 mission cost estimate is a combination of high-level parametric and analog techniques and incorporates a wide range of uncertainty in the estimating process. No adjustments were made to remove the historical cost of manifested risk from the heritage data underlying the baseline estimate. Therefore, before reserves are applied, the estimated costs already include a historical average of the cost of risk. This approach is appropriate for capturing risk and uncertainty commensurate with early formulation stages of a mission. The following describes the basis of estimate for each element.

WBS 1, 2, 3: Project Management, Systems Engineering, Mission Assurance (PMSEMA). Because these functions depend on multiple mission- and organization-specific characteristics [Hahn 2014], cost analogies to comparable historical missions are preferred over cost-model output, which does not take the mission into account. Existing analyses demonstrate that hardware costs are a reliable predictor of these critical mission function costs. APL has conducted thorough and rigorous analyses of PMSEMA costs, both for historical APL missions and for analogous missions. The PMSEMA estimate for Calypso relies on APL's analysis of historical PMSEMA practices on Van Allen Probes (VAP), Parker Solar Probe (PSP), and New Horizons (NH). VAP and PSP, in particular, include costs associated with current NASA requirements (e.g., earned value management system (EVMS), 7120.5E). Calypso's total mission PMSEMA cost is 15.9% of the flight system (payload + spacecraft+ I&T). This percentage is allowed to vary along with hardware costs as part of the mission cost risk analysis, discussed below, to capture uncertainty (particularly given CML-4 level).

Payload	Analogy Instrument	Analogy	NICM	SEER	Average
Narrow Angle Camera (NAC)	NH LORRI	$15,517	$18,980	$18,288	$17,595
Mapping Imaging Spectrometer (Vis/NIR)	NH RALPH	$48,100	$15,135	$15,284	$48,100
Energetic Plasma Detector (EPD)	MMS EIS	$7,907	$4,143	$1,971	$4,673
Ion Electrostatic Analyzer (I-ESA)	NH SWAP	$10,525	$5,051	$2,872	$6,149
Radio Science Experiment (RS)	NH Rex	$1,133	$1,741	$1,074	$1,316
Magnetometer (MAG) x2	MESSENGER MAG	$3,164	$5,680	$6,882	$5,242
Mag Boom	VAP Boom	$3,049	N/A	N/A	$3,049
Dust Counter (D-Count)	NH SDC	N/A	$2,801	$1,428	$2,115
Ultraviolet Imaging Spectrometer (UVIS)	NH ALICE	$11,710	$8,527	$7,740	$9,326
Electron Electrostatic Analyzer (E-ESA)	PSP SPAN-B	N/A	$4,258	$5,872	$5,065
Total					**$102,631**

Exhibit 5-3. *WBS 5 (payload) costs in FY$25K.*

Spacecraft	TruePlanning	SEER	Average	Cross-Check	Notes
Telecomm	$39,222	$40,324	$39,773	$43,977	Calypso dual-band communications subsystem is cross-checked against PSP, also dual band.
CDH/Avionics	$40,104	$38,876	$39,490	$33,93	Calypso IEM is modeled after PSP avionics. PSP has a sufficient capability for the processing requirements of Calypso.
Power	$41,087	$40,261	$40,674	$41,591	Power is cross-checked with PSP, a recent development.
Structure	$20,517	$14,193	$20,745	$15,773	Historically, APL's structure subsystem is 14% of S/C hardware costs. The average is replaced with this and cross-checked with New Horizons (80 kg less than Calypso)
Attitude/GNC	$15,179	$14,874	$15,026	$15,065	TruePlanning and SEER average compared to New Horizons.
Thermal	$2,078	$4,624	$3,351	$2,174	TruePlanning and SEER average compared to New Horizons.
Propulsion	$8,100	$8,100	$8,100	$10,670	Propulsion ROM compared to New Horizons.
Harness	$1,447	$2,087	$1,767	$1,446	TruePlanning and SEER average compared to New Horizons.
Flight Software (FSW)	$26,802	Included	$26,802	$26,802	PSP actuals used.
Component Engineering	$19,769	$19,769	$19,769	$19,769	New Horizons actuals used.
Total	**$214,307**	**$183,108**	**$215,499**	**$211,171**	

Exhibit 5-4. *WBS 6 (spacecraft) costs in FY$25K.*

WBS 4: Science. This element covers the managing, directing, and controlling of the science investigation. It includes the costs of the principal investigator (PI), project scientist (PS), science team members, and activities. The Phase A–D and E–F science estimate is an analogous estimate based on the cost per month of NH, MESSENGER, Cassini, Dragonfly, OSIRIS-Rex, and Juno. NH is the predecessor mission to Calypso; MESSENGER is APL's most recent historical data point for planetary orbital science; and Cassini is a recently completed outer planets flagship mission. The analogy costs are representative of expenditures for science on a typical New Frontiers or Flagship mission. The estimate reflects the manpower needed to create various data products as well as to ensure closure to science objectives.

WBS 5: Payload. The WBS 5 estimate includes a science payload of 10 instruments (9 unique), a magnetometer boom, and payload-level PMSEMA (Ex. 5-3). The 8.2% cost-to-cost factor for estimating payload PMSEMA costs is based on the VAP, NH, MESSENGER, and PSP payload suite cost data with PMSEMA costs estimated as a percentage of the payload hardware. Technical management and systems engineering costs for individual instruments are carried in their respective instrument development costs.

Given the early design phase, multiple approaches are used to estimate each instrument to capture the potential range in cost. This includes two parametric estimates that rely on different sets of input variables (SEER Space and NICM 9), and historical analogous costs to specific heritage instruments where available. An average of the historical analogy and two parametric estimates is used as the point estimate to prevent estimate bias (high or low). To maintain conservatism given the early design phase, the analogy estimate is selected for the Vis/NIR Imaging Spectrometer. These estimates are subject to a cost risk analysis (discussed below) to further quantify uncertainty.

WBS 6: Spacecraft. The WBS 6 estimate includes the spacecraft bus and a next generation RTG mod 0 (Ex. 5-6). Spacecraft PMSEMA is carried in WBS 1, 2, and 3 consistent with APL in-house builds [Hahn 2015]. The basis of estimate relies primarily on parametric models. The exception to this is the propulsion system,

estimated via a ROM by a propulsion subject-matter expert based on recent IMAP experience, as well as the RTG, in accordance with PMCS guidelines. An average of two parametric estimates is used as the point estimate to mitigate estimate bias (high or low). SEER Space is one of the primary estimating methodologies because it was designed specifically for missions in early formulation stages. TruePlanning is also utilized as it provides a cost estimate at the component level. No major technology development is required for the spacecraft. The two parametric estimates are within 15% of each other (which is a reasonable range given different input variables). Cross-checks are shown in the table. The $50M RTG is added to the total to complete the WBS 6 estimate.

WBS 7 & 9: Mission Operations and Ground Data Systems (GDS). The Calypso mission operations estimate includes mission operations planning and development, network security, data processing, and mission management. The pre- and post-launch mission operations estimate are based on the cost per month of NH, PSP, and OSIRIS-Rex. NH and PSP represent typical APL expenditure on pre-launch mission operations for projects of comparable scope and complexity. OSIRIS-Rex is included due to similar navigation needed for Calypso. The GDS estimate is a bottoms-up estimate (BUE) with NH testbed actuals added. The Calypso ground data system provides full life cycle support for subsystem test, observatory I&T, hardware simulator control, and flight operations. The cost estimate is based on extensive reuse of PSP, Dragonfly, and DART ground software via APL's Mission Independent Ground Software (MIGS) as well as use of the existing Building 21 Mission Operations Center (MOC).

WBS 8: Launch Vehicle and Services. The mission requires a launch vehicle that does not correspond with any of the options currently described in the PMCS ground rules. As such, the figures used in this estimated are based on an evaluation of current best estimates of the cost of the capability that will be required. The price of a LV with Falcon Heavy Expendable-type capabilities, based on past pricing to NASA missions of EELVs, would be at least $210M for a launch using a standard sized fairing. The price to add an upper stage would likely be no more than $40M. NEPA and nuclear launch approval costs are covered by the cost of the RTGs in WBS 6. The $26M RTG surcharge is included.

WBS 10: System Integration and Testing (I&T). This element covers the efforts to assemble and test the spacecraft and instruments. The Calypso I&T effort is estimated as 12.7% of the hardware. This percentage is based on a detailed analysis of cost actuals from previous APL missions, including MESSENGER, NH, STEREO, VAP, and PSP. This percentage is allowed to vary along with hardware costs as part of the mission cost risk analysis to capture the risk historically manifested during I&T.

Deep Space Network (DSN). This element provides for access to the DSN infrastructure needed to transmit and receive mission and scientific data. Mission charges are estimated using the Jet Propulsion Laboratory (JPL) DSN Aperture Fee tool. The DSN cost estimate covers pre- and post-contact activity for each linkage.

5.5 Confidence & Cost Reserves

The cost risk ranges by major WBS element as inputs for the Calypso probabilistic cost risk analysis to quantify total cost risk are found in Ex. 5-5 and are described below.

WBS	Cost Element	Project Estimate	70th Percentile
1,2,3	Mission PMSEMA	$67,444	$90,655
4	Science	$28,255	$35,319
5	Payload	$110,996	$154,879
6	Spacecraft	$265,499	$351,028
7	Mission Ops	$23,143	$28,929
8	Launch Vehicle	$276,000	$276,000
9	Ground Data System	$24,021	$30,026
10	I&T	$47,680	$64,250

Exhibit 5-5. *Inputs to cost distributions in FY$25K.*

PMSEMA. Given the use of cost-to-cost factors to estimate these functions, both the CER and underlying cost drivers are allowed to range so that all sources of uncertainty can be quantified.

Science, Ground Data Systems & Mission Ops. These are low-risk cost elements but are subject to cost growth as part of the cost risk analysis.

Payload. Given that the point estimate is an average of two parametric models and a historical analogy for each of the 10 instruments, the highest value of the three primary estimate inputs is used to inform the Calypso payload risk model to capture the uncertainty given the CML-4-level design phase.

Spacecraft. Each subsystem is subject to a data-driven risk analysis based on historical APL cost growth. Mass input also varies in the SEER space model consistent with early design programs to 30% over current best estimate.

Integration &Test. I&T as a percentage of the payload and spacecraft from the point estimate is used to inform the risk analysis, allowing I&T to vary with hardware cost.

Per the PMCS ground rules, the estimate includes unencumbered cost reserves of 50% of the estimated costs of all Phase A–D elements except for the launch vehicle. A probabilistic cost risk analysis shows 79% confidence that the Phase A–D mission is achievable within the estimated costs of this study (see Ex. 5-6 and Ex. 5-7). The high confidence level is driven primarily by the large cost reserves for this pre-proposal concept. Given a typical competitive pre-Phase A NASA environment with 25% reserves on Phase A–D elements, the probabilistic cost risk analysis shows 65% confidence that the Phase A–D mission would be achievable. A 50th- to 70th-percentile confidence level is expected and reasonable for a pre-Phase A concept with this level of reserves.

Description	Value (FY$25K)	Confidence
Point Estimate	$843,037	46%
Mean	$937,631	
Standard Deviation	$303,856	
Cost Reserves	$283,519	
PIMMC	$1,152,556	79%

Exhibit 5-6. *Cost-risk analysis.*

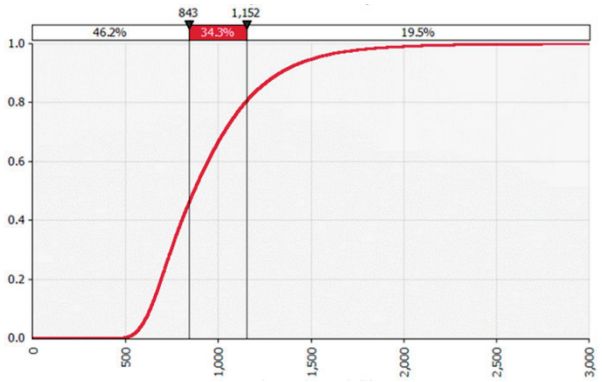

Exhibit 5-7. *S-curve summary of cost-risk analysis.*

A coefficient of variation (standard deviation/mean) of approximately 33% indicates appropriate levels of conservatism given the early formulation phase. The model confirms the point estimate and provides a reasonable basis for the Calypso CML-4 study.

.

Appendix A: Additional Technical Details

Mission Power Summaries

Power Budget	Launch Post Sep (PS-H)	Spin Up/Down/Precess (AS-N)	Spin Cruise (PS-H)	Spin TCM Pre-Burn (AS-N)	Active Spin TCM Burn (AS-T)	3-Axis TCM Pre-Burn (3A-N)	3-Axis TCM Burn (3A-T)	Downlink 2 CDH Processors (3A-N, AS-N)	Dual TWTA Downlink (PS-N)	Downlink w/PEPSSI & SWAP (3A-N, AS-N)	3-Axis Science, Thruster Inhibit (3A-E) w/MAG,SWEAP, MMSEIS,SWAPI, REX	3-Axis Science (3A-E) w/RALPH, LORRI	3-Axis Science (3A-E) w/Alice, REX	Precess (AS-N)	Earth Acq TWTA (AS-EA)	Sun Acq IMU (AS-SA)	Sun Acq TWTA (AS-SA)
Science Instruments	0.0	0.0	30.4	0.0	0.0	0.0	0.0	0.0	0.0	4.8	13.3	12.6	6.6	0.0	0.0	0.0	0.0
Avionics	26.4	20.2	13.2	20.2	20.2	20.2	20.2	33.4	13.2	20.2	16.7	23.7	23.7	20.2	20.2	20.2	20.2
Power System	18.7	18.7	18.7	18.7	18.7	18.7	18.7	18.7	18.7	18.7	18.7	18.7	18.7	18.7	18.7	18.7	18.7
Telecommunications	54.2	17.5	54.2	17.5	17.5	17.5	17.5	54.2	86.7	54.2	17.5	17.5	17.5	17.5	54.2	21.4	58.2
Attitude Control	0.0	38.0	0.0	38.0	36.8	38.0	36.8	6.0	0.0	6.0	38.0	38.0	38.0	38.0	6.0	38.9	6.9
Propulsion	1.4	28.1	1.4	37.0	47.1	37.0	47.1	28.1	1.4	14.7	28.1	28.1	28.1	28.1	28.1	28.1	28.1
Thermal Required Loads	4.8	0.0	4.8	0.0	0.0	0.0	0.0	0.0	4.8	0.0	0.0	0.0	0.0	0.0	0.0	0.0	0.0
Harness	3.4	4.8	4.8	4.8	4.8	4.8	4.8	4.8	4.8	4.8	4.8	4.8	4.8	4.8	4.8	4.8	4.8
Transient Allocation Peak Power above steady state (<200ms)	0.0	15.0	15.0	15.0	15.0	15.0	15.0	15.0	15.0	15.0	15.0	15.0	15.0	15.0	15.0	15.0	15.0
Total Load	**108.9**	**142.3**	**142.5**	**151.2**	**160.1**	**151.2**	**160.1**	**160.2**	**144.6**	**138.4**	**152.1**	**158.4**	**152.4**	**142.3**	**147.0**	**147.1**	**151.9**

Exhibit A-1. *Uranian System Investigation Peak Power Levels.*

Power Budget	Spin Up/Down/Precess (AS-N)	Spin Cruise (PS-H)	3-Axis TCM Pre-Burn (3A-N)	3-Axis TCM Burn (3A-T)	Downlink 2 CDH Processors (3A-N, AS-N)	Downlink w/PEPSSI & SWAP (3A-N, AS-N)	3-Axis Science, Thruster Inhibit (3A-E) w/MAG,SWEAP, MMSEIS,SWAPI, REX	3-Axis Science, Thruster Inhibit (3A-E) w/MAG,SWEAP, MMSEIS,SWAPI, REX	3-Axis Science (3A-E) w/RALPH	3-Axis Science (3A-E) w/LORRI	Precess (AS-N)	Earth Acq TWTA (AS-EA)	Sun Acq IMU (AS-SA)	Sun Acq TWTA (AS-SA)
Science Instruments	0.0	9.8	0.0	0.0	0.0	0.0	11.1	4.8	7.1	5.5	0.0	0.0	0.0	0.0
Avionics	16.7	13.2	16.7	16.7	16.7	16.7	16.7	16.7	20.2	20.2	16.7	16.7	16.7	16.7
Power System	18.7	18.7	18.7	18.7	18.7	18.7	18.7	18.7	18.7	18.7	18.7	18.7	18.7	18.7
Telecommunications	11.1	54.2	11.1	11.1	54.2	54.2	11.1	11.1	11.1	11.1	17.5	54.2	21.4	58.2
Attitude Control	38.0	0.0	38.0	36.8	6.0	6.0	38.0	38.0	38.0	38.0	38.0	6.0	38.9	6.9
Propulsion	14.7	1.4	22.3	32.4	14.7	14.7	13.4	13.4	13.4	13.4	14.7	14.7	14.7	14.7
Thermal Required Loads	0.0	4.8	0.0	0.0	0.0	0.0	0.0	0.0	0.0	0.0	0.0	0.0	0.0	0.0
Harness	4.8	4.8	4.8	4.8	4.8	4.8	4.8	4.8	4.8	4.8	4.8	4.8	4.8	4.8
Transient Allocation Peak Power above steady state (<200ms)	15.0	15.0	15.0	15.0	15.0	15.0	15.0	15.0	15.0	15.0	15.0	15.0	15.0	15.0
Total Load	**119.1**	**121.9**	**126.7**	**135.5**	**130.1**	**130.1**	**128.8**	**122.5**	**128.3**	**126.7**	**125.4**	**130.1**	**130.2**	**134.9**

Exhibit A-2. *G!kún‖'hòmdímà / G!ò'é !Hú Investigation Peak Power Levels.*

Power Budget	KBO#2 TCM Pre-Burn	KBO#2 TCM Maneuver Spin	KBO#2 TCM Maneuver 3-Axis	KBO#2 3-Axis Science	KBO#2 Downlink Spin	KBO#2 Downlink 3-Axis	KBO#2 Spin Up/Down/ Precess Pre-Burn	KBO#2 Spin Up/Down/ Precess	KBO#2 Cruise	Spin Sun Safe	Spin Earth Safe	3-Axis Earth Safe, Gyro ON, Downlink/TWTA OFF
Science Instruments	0.0	0.0	0.0	0.0	0.0	0.0	0.0	0.0	5.0	0.0	0.0	0.0
Avionics	13.2	13.2	13.2	13.2	13.2	13.2	13.2	13.2	13.2	13.2	13.2	13.2
Power System	18.7	18.7	18.7	18.7	18.7	18.7	18.7	18.7	18.7	18.7	18.7	18.7
Telecommunications	16.3	16.3	16.3	16.3	53.1	53.1	16.3	16.3	13.7	53.1	53.1	16.3
Attitude Control	6.0	36.8	36.8	38.0	0.0	6.0	6.0	38.0	6.9	6.9	8.1	38.0
Propulsion	10.3	20.3	1.4	1.4	1.4	1.4	1.4	1.4	1.4	1.4	1.4	1.4
Thermal Required Loads	0.0	0.0	0.0	0.0	4.8	0.0	0.0	0.0	0.0	0.0	0.0	0.0
Harness	2.2	2.8	2.5	2.5	2.6	2.6	2.0	2.5	2.1	2.6	2.6	2.5
Transient Allocation Peak Power above steady state (<200ms)	15.0	15.0	15.0	15.0	15.0	15.0	15.0	15.0	15.0	15.0	15.0	15.0
Total Load	**81.6**	**123.1**	**103.8**	**105.1**	**108.6**	**109.8**	**72.5**	**105.1**	**75.9**	**110.7**	**111.9**	**105.1**

Exhibit A-3. *KBO Extended Mission Peak Power Levels.*

Appendix B: Acronyms & Abbreviations

ACS	Attitude Control System
AO	Announcement of Opportunity
AU	Astronomical Unit
APL	Johns Hopkins Applied Physics Laboratory
APXS	Alpha Particle X-Ray Spectrometer
BELA	BepiColombo Laser Altimeter
BOE	Basis of Estimate
BOL	Beginning of Life
BUE	Bottom-Up Estimate
C/A	Close (Closest) Approach
C&DH	Command and Data Handling
Catbed (Heaters)	Catalyst Bed (Heaters)
CBE	Current Best Estimate
CDR	Critical Design Review
CER	Cost Estimating Relationship
cFE	Core Flight Executive
CFDP	CCSDS File Delivery Protocol
CFEPS	Canada-France Ecliptic Plane Survey
CheMin	Chemistry and Mineralogy
CG	Center of Gravity
CLPS	Commercial Lunar Payload Services
CML	Concept Maturity Level
CMOS	Complementary Metal Oxide Semiconductor
COTS	Commercial Off the Shelf
ΔV	Delta (Change in) Velocity
D-Count	Dust Counter
DART	Double Asteroid Redirection Test
DC/DC	Direct-Current to Direct-Current (Converter Card)
DD	Dust Detector
DMA	Direct Memory Access
DSN	Deep Space Network
DSS	Digital Sun Sensor
DTE	Direct to Earth

DTM	Digital Terrain Model
DVR	Digital Video Recorder
E-ESA	Electron Electrostatic Analyzer
EC	Electrical Conductivity
EFH	Expendable Falcon Heavy
EOL	End of Life
EPC	Electronic Power Conditioner
EPD	Energetic Particle Detector
ESA	European Space Agency
EVMS	Earned Value Management System
FOV	Field of View
FPGA	Field-Programmable Gate Array
FSS	Fine Sun Sensor
FSW	Flight Software
FY	Fiscal Year
G&C	Guidance and Control
GDS	Ground Data System
HGA	High-Gain Antenna
I-IESA	Ion Electrostatic Analyzer
I&T	Integration and Test
I^2C	Inter-Integrated Circuit
IBR	Integrated Baseline Review
IEM	Integrated Electronics Module
IIF	Instrument Interface (Card)
IMU	Inertial Measurement Unit
IR	Infrared
JGA	Jupiter Gravity Assist
JPL	Jet Propulsion Laboratory
JSC	Johnson Space Center
KBO	Kuiper Belt Object
LEISA	Linear Etalon Imaging Spectral Array
LEOP	Launch and Early Operations Phase
LGA	Low-Gain Antenna
LNA	Low-Noise Amplifiers
LORRI	(New Horizons) Long Range Reconnaissance Imager

LRD	Launch Readiness Date
LRM	Low-Reflectance Material
LRR	Launch Readiness Review
LV	Launch Vehicle
LVS	Low-Voltage Sensor
MA	Mission Assurance
MAG	Magnetometer
MatISSE	Maturation of Instruments for Solar System Exploration
MEL	Master Equipment List
MEOP	Maximum Expected Operating Pressure
MER	Mars Exploration Rovers
MESSENGER	MErcury Surface, Space ENvironment, GEochemistry, and Ranging
MEV	Maximum Expected Value
MGA	Medium-Gain Antenna
MIGS	Mission Independent Ground Software
MIMU	Miniature Inertial Measurement Unit
MLI	Multi-Layer Insulation
MOC	Mission Operations Center
MON-3	Mixed Oxides of Nitrogen (Nitrogen Tetroxide)
MOps	Mission Operations
MOR	Mission Operations Review
MRAM	Magnetoresistive Random-Access Memory
MRR	Mission Readiness Review
MSL	Mars Science Laboratory
MUX	Multiplexer
MVIC	Multispectral Visible Imaging Component (of the Vis/NIR)
NAC	Narrow Angle Camera
NASA	National Aeronautics and Space Administration
NH	New Horizons
NICM	NASA Instrument Cost Model
NIR	Near Infrared
NPR	NASA Procedural Requirement
NRE	Non-Recurring Engineering
ORR	Operational Readiness Review
OSIRIS-REx	Origins, Spectral Interpretation, Resource Identification, Security-Regolith EXplorer

PDR	Preliminary Design Review
PER	Pre-Environmental Review
PDB	Propulsion Diode Boxes
PDU	Power Distribution Unit
PM	Project Management
PMCS	Planetary Mission Concept Studies
PMSEMA	Project Management, Systems Engineering, Mission Assurance
PPS	Pulse Per Second
PPU	Power Processing Unit
PSP	Parker Solar Probe
PSR	Pre-Ship Review
PSU	Power Switching Unit
RDM	Radiation Design Model
RIO	Remote Input/Output
RIU	Remote Interface Unit
ROM	Rough Order of Magnitude
RPM	Rotations per Minute
RS	Radio Science
RTG	Radioisotope Thermoelectric Generator
RW	Reaction Wheel
S/C	Spacecraft
SBC	Single Board Computer
SCIF	Spacecraft Interface
SE	Systems Engineering
SEER	System Evaluation and Estimation of Resources
SEIS-SP	Seismic Experiment for Internal Structure-Short Period
SEP	Solar Electric Propulsion
SIR	System Integrations Review
SMSR	Safety and Mission Success Review
SOR	Science Operations Review
SPHERE	Spectro-Polarimetric High-contrast Exoplanet REsearch
SPS	Sun Pulse Sensor
SRAM	Static Random-Access Memory
SRR	System Requirements Review
SRU	Shunt Regulator Unit

SSR	Solid-State Recorder
SWAP	(New Horizons) Solar Winds Around Pluto
SWAPI	(IMAP) Solar Winds and Pickup Ions
TAC	Thruster/Actuator Card
TCM	Trajectory Correction Maneuver
TID	Total Ionizing Dose
TOF	Time of Flight
TRL	Technology Readiness Level
TT&C	Tracking, Telemetry and Control
TWTA	Travelling Wave Tube Amplifier
UMOD	Uranian Model
USO	Ultra-Stable Oscillator
UVIS	Ultraviolet Imaging Spectrometer
VAP	Van Allen Probes
Vis/NIR	Visible and Near-Infrared (Imaging Spectrometer Instrument)
VLT	Very Large Telescope
WBS	Work Breakdown Structure

Appendix C: References

Anderson, B.J. et al. (2007). The Magnetometer Instrument on MESSENGER", *Space Sci. Rev. 131*, 417–450. https://doi.org/10.1007/s11214-007-9246-7

Barkume, K.M., M.E. Brown, and E.L. Schaller (2008). Near-Infrared Spectra of Centaurs and Kuiper Belt Objects. *Astron. J., 135,* 55–67. doi:10.1088/0004-6256/135/1/55

Benedetti-Rossi, G. et al. (2016). Results from the 2014 November 15th Multi-chord Stellar Occultation by the TNO (229762) 2007 UK126. *Astron. J.,152.* doi:10.3847/0004-6256/152/6/156

Bierson, C.J. and F. Nimmo (2019). Using the density of Kuiper Belt Objects to constrain their composition and formation history. *Icarus, 326*, 10–17. doi:10.1016/j.icarus.2019.01.027

Brown, M.E., E.L. Schaller, and W.C. Fraser (2012). Water Ice in the Kuiper Belt. *Astron. J., 143,* doi:10.1088/0004-6256/143/6/146

Buckley, M. (2021). Johns Hopkins APL Technology Helps Mars Mission Phone Home, Johns Hopkins APL Website (https://www.jhuapl.edu/NewsStory/210318-Hope-Mars-mission), accessed 7 May 2021.

Carrozzo, F.G., M.C. De Sanctis, A. Raponi, E. Ammannito, J.C. Castillo-Rogez, et al.(2018). Nature, formation, and distribution of carbonates on Ceres. *Science Advances 4*, e1701645. doi:10.1126/sciadv.1701645

Carry, B. et al. (2021). Evidence for differentiation of the most primitive small bodies. arXiv e-prints.

Castillo-Rogez, J.C., M. Hesse, et al. (2019). Conditions for the preservations of brines inside Ceres. *Geophys. Res. Lett., 46,* 1963-1972. https://doi.org/10.1029/2018GL081473

Castillo-Rogez, J.C. et al., (2020). Ceres: Astrobiological target and possible ocean world. *Astrobiology,* 269-291. https://doi.org/10.1089/ast.2018.1999

Castillo, J.C. (2020). Future exploration of Ceres as an ocean world. *Nat. Astron., 4,* 732-734. https://doi.org/10.1038/s41550-020-1181-5

Castillo-Rogez, J.C. et al., (submitted). Role of supervolatiles in driving ocean salinity and electrical conductivity in ocean worlds. *Geophys. Res. Lett.*

Cheng, A.F. et al. (2008). Long-Range Reconnaissance Imager on New Horizons, *Space Sci. Rev. 140*, 189–215. https://doi.org/10.1007/s11214-007-9271-6

Cochrane, C.J., T.A. Nordheim, S.D. Vance, M. Styczinski, K. Soderlund, C.M. Elder, et al., (2021). In search of subsurface oceans within the moons of Uranus. Lunar and Planetary Science Conference 52, abstract #1559.

Connerney, J.E.P., M.H. Acuna, and N.F. Ness (1987). The magnetic field of Uranus, *J. Geophys. Res. 92*, 15329-15336,

Choblet, G., G. Tobie, C. Sotin, M. Behounkova, O. Cadek, F. Postberg, and O. Soucek (2017). Powering prolonged hydrothermal activity inside Enceladus. *Nat. Astron., 1,* 841-847. doi: 10.1038/s41550-017-0289-8.

Coustenis, A., Rodrigo, R., Spohn, T., L'Haridon, J. 2020. Editorial to the Topical Collection: Ocean Worlds. Space Science Reviews 216. doi:10.1007/s11214-020-00672-z

de Sanctis, M.C. et al. (2015). Ammoniated phyllosilicates with a likely outer Solar System origin on (1) Ceres. *Nature, 528,* 241–244. doi:10.1038/nature16172

Fernandez-Valenzuela, E. et al. (2019). The Changing Rotational Light-curve Amplitude of Varuna and Evidence for a Close-in Satellite. *Astron. J., 883*, L21. doi:10.3847/2041-8213/ab40c2

Fountain, G.H. et al. (2008).The New Horizons Spacecraft, *Space Sci. Rev. 140*, 23–47. https://doi.org/10.1007/s11214-008-9374-8

Garrett, H.B., L.M. Martinez-Sierra, and R.W. Evans (2015). The JPL Uranian Radiation Model (UMOD), *JPL Publication 15-7*, 55. California Institute of Technology, Pasadena, CA, http://hdl.handle.net/2014/45462

Glein, C.R. and J.H. Waite (2020). The Carbonate Geochemistry of Enceladus' Ocean, *Geophys. Res. Lett., 47*, 3. e2019GL085885. https://doi.org/10.1029/2019GL085885

Gomes, R.S., J.A. Fernàndez, T. Gallardo, and A. Brunini (2008). The Scattered Disk: Origins, Dynamics, and End States. *The Solar System Beyond Neptune*. University of Arizona Press, Tucson, AZ. 259-273

Grundy, W.M., K.S. Noll, M.W. Buie, S.D. Benecchi, D. Ragozzine, and H.G. Roe (2019). The mutual orbit, mass, and density of transneptunian binary G!kún‖'hòmdímà (229762 2007 UK126). *Icarus, 334,* 30–38. doi:10.1016/j.icarus.2018.12.037

Hahn, M. (2014) Higher Fidelity Estimating: Program Management, Systems Engineering, & Mission Assurance. *2014 NASA Cost Symposium.*

Hahn, M. (2015) In-House Build Efficiencies: PM, SE, & MA. *2015 NASA Cost Symposium.*

Hendrix, A.R., T.A. Hurford, et al. (2019) The NASA Roadmap to Ocean Worlds. *Astrobiology, 19.* doi:10.1089/ast.2018.1955

Herbert, F. (2009). Aurora and magnetic field of Uranus, *J. Geophys. Res. 114*, A11206. doi:10.1029/2009JA014394

Horányi, M., V. Hoxie, D. James, et al. (2008). The Student Dust Counter on the New Horizons Mission, *Space Sci. Rev. 140*, 387–402. https://doi.org/10.1007/s11214-007-9250-y

Hussmann, H., F. Sohl, and T. Spohn (2006) Subsurface oceans and deep interiors of medium0sized outer planet satellites and large trans-neptunian objects. *Icarus, 185,* 258-273. doi:10.1016/j.icarus.2006.06.005

Iess, L., D.J. Stevenson, M. Parisi, D. Hemingway, R.A. Jacobson, J.I. Lunine, et al. (2014) The gravity field and interior structure of Enceladus, *Science, 344*, 78-80. doi: 10.1126/science.1250551

Kamata, S., F. Nimmo, Y. Sekine, K. Kuramoto, N. Noguchi, J. Kimura, and A. Tani (2019) Pluto's ocean is capped and insulated by gas hydrates, *Nat. Geosci., 12,* 407-410. https://doi.org/10.1038/s41561-019-0369-8

Kasper, J.C., R. Abiad, G. Austin, et al. (2016) Solar Wind Electrons Alphas and Protons (SWEAP) Investigation: Design of the Solar Wind and Coronal Plasma Instrument Suite for Solar Probe Plus, *Space Sci. Rev. 204,* 131–186. https://doi.org/10.1007/s11214-015-0206-3

Kavelaars, J.J. et al. (2009). The Canada-France Ecliptic Plane Survey-L3 Data Release: The Orbital Structure of the Kuiper Belt. *Astron. J., 137*, 4917–4935. doi:10.1088/0004-6256/137/6/4917

Kegerreis, J.A.et al. (2018). Consequences of Giant Impacts on Early Uranus for Rotation, Internal Structure, Debris, and Atmospheric Erosion. *Astron. J., 861* 52. doi:10.3847/1538-4357/aac725

Kirchoff, M. and L. Dones (2018) Impact crater distributions of the Uranian satellites: new constraints for outer solar system bombardement. *42nd COSPAR Scientific Assembly*. P. Abst. #B5.4-0007-18, Pasadena, CA: COSPAR.

Lacerda, P. and J. Luu. (2006). Analysis of the Rotational Properties of Kuiper Belt Objects. *Astron. J. 131*, 2314–2326. doi:10.1086/501047

Lauer, T.R., H.B. Throop, M.R. Showalter, H.A. Weaver, S.A. Stern, J.R. Spencer, et al. (2019). The New Horizons and Hubble Space Telescope search for rings, dust, and debris in the Pluto/Charon system. Pluto System After New Horizons, LPI Contribution No. 2133, Laurel, MD, 2019 July 14-18, 7041 (Abstract).

Lineweaver, C.H. and M. Norman (2010). The Potato Radius: a Lower Minimum Size for Dwarf Planets. *Australian Space Science Conference Series: Proceedings of the 9th Australian Space Science Conference*, eds W. Short & I. Cairns, National Space Society of Australia. https://arxiv.org/ftp/arxiv/papers/1004/1004.1091.pdf

Marchi, S. et al. (2016). The missing large impact craters on Ceres. *Nat. Commun., 7,* 12257. doi:10.1038/ncomms12257

Mauk, B.H., J.B. Blake, D.N. Baker et al. (2016). The Energetic Particle Detector (EPD) Investigation and the Energetic Ion Spectrometer (EIS) for the Magnetospheric Multiscale (MMS) Mission, *Space Sci. Rev. 199,* 471–514. doi:10.1007/s11214-014-0055-5

McCleskey, R.B., D.K. Nordstrom, and J.N. Ryan (2012). Comparison of electrical conductivity calculation methods for natural waters, *Limnol. Oceanogr.-Meth*., *10,* 952-967, https://doi.org/10.4319/lom.2012.10.952

McComas, D., F. Allegrini, F. Bagenal, et al. (2008). The Solar Wind Around Pluto (SWAP) Instrument Aboard New Horizons, *Space Sci. Rev. 140,* 261–313. doi:10.1007/s11214-007-9205-3

McNutt, R.L., S.A. Livi, R.S. Gurnee, et al. (2008). The Pluto Energetic Particle Spectrometer Science Investigation (PEPSSI) on the New Horizons Mission", *Space Sci. Rev. 140,* 315–385. doi:10.1007/s11214-008-9436-y

Mousis O., A. Aguichine, R. Helled, P.G.J. Irwin, and J.I. Lunine J. I. (2020). The role of ice lines in the formation of Uranus and Neptune, *Phil. Trans. R. Soc.* A.3782020010720200107 http://doi.org/10.1098/rsta.2020.0107

Morbidelli, A., D. Nesvorný, W.F. Bottke, and S. Marchi (2021). A re-assessment of the Kuiper belt size distribution for sub-kilometer objects, revealing collisional equilibrium at small sizes. *Icarus, 356.* doi:10.1016/j.icarus.2020.114256

Nesvorný, D. and A. Morbidelli (2012). Statistical study of the early Solar System's instability with four, five, and six giant planets. *Astron. J., 144,* 117. doi: 10.1088/0004-6256/144/4/117

Nesvorný, D. and D. Vokrouhlický (2016). Neptune's Orbital Migration Was Grainy, Not Smooth. *Astron. J., 825*, 94. doi: 10.3847/0004-637x/825/2/94

Nesvorný, D., R. Li, A.N. Youdin, J.B. Simon, and W.M. Grundy (2019). Trans-Neptunian binaries as evidence for planetesimal formation by the streaming instability. *Nat. Astron., 3*, 808–812. doi:10.1038/s41550-019-0806-z

Nesvorný, D., D. Vokrouhlický, W.F. Bottke, H.F. Levison, and W.M. Grundy (2020). Very Slow Rotators from Tidally Synchronized Binaries. *Astrophys. J. 893,* L16. doi:10.3847/2041-8213/ab8311

Nesvorný, D. et al. (2021). Binary Planetesimal Formation from Gravitationally Collapsing Pebble Clouds. *Planet. Sci. J., 2,* 27. doi:10.3847/PSJ/abd858

Neveu, M. and A.R. Rhoden (2019). Evolution of Saturn's mid-sized moons, *Nat. Astron., 3*, 543-552. https://doi.org/10.1038/s41550-019-0726-y

Parkinson W.D. (1983) *Introduction to Geomagnetism,* Scottish Academic Press, London, 433 pp.

Peterson, G., F. Nimmo, and P. Schenk (2015). Elastic thickness and heat flux estimates for the uranian satellite Ariel. *Icarus, 250,* 116-122. https://doi.org/10.1016/j.icarus.2014.11.007

Postberg, F., J. Schmidt, J. Hillier, S. Kempf, and R. Srama, R. (2011) .A salt-water reservoir as a source of compositionally stratified plume on Enceladus, *Nature 474*, 620-622. doi:10.1038/nature10175

Prieto-Ballesteros, O. and J.S. Kargel (2005). Thermal state and complex geology of a heterogeneous salty crust of Jupiter's satellite, Europa, *Icarus 173*, 212-221. doi:10.1016/j.icarus.2004.07.019

Raymond, C.A. et al. (2020). Impact-driven mobilization of deep crustal brines on dwarf planet Ceres, *Nat. Astron. 4,* 741-747. doi:10.1038/s41550-020-1168-2

Rebello, L.R.R., T. Siepman, and S. Drexler (2020). Correlations between TDS and electrical conductivity for high-salinity formation brines characteristic of South Atlantic pre-salt basins *Water SA 46,* 602-609, https://doi.org.10.17159/wsa/2020.v46.i4.9073

Reuter, D.C., S.A. Stern, J. Scherrer, et al. (2008). Ralph: A Visible/Infrared Imager for the New Horizons Pluto/Kuiper Belt Mission", *Space Sci. Rev. 140,* 129–154. doi:10.1007/s11214-008-9375-7

Schindler, K. et al. (2017). Results from a triple chord stellar occultation and far-infrared photometry of the trans-Neptunian object (229762) 2007 UK126. *Astron. Astrophys. 600.* doi:10.1051/0004-6361/201628620

Schenk, P.M., and J.M. Moore (2020). Topography and geology of Uranian mid-sized icy satellites in comparison with Saturnian and Plutonian satellites, *Phil. Trans. R. Soc.* A.3782020010220200102, http://doi.org/10.1098/rsta.2020.0102

Schmidt, C. and C. Manning (2017). Pressure-induced ion pairing in MgSO4 solutions: Implications for the oceans of icy worlds, *Geochemical Perspectives Letters, 3*, 66–74. doi:10.7185/geochemlet.1707

Sheppard, S.S. and D.C. Jewitt. (2002). Time-resolved Photometry of Kuiper Belt Objects: Rotations, Shapes, and Phase Functions. *The Astronomical Journal 124*, 1757–1775. doi:10.1086/341954

Smith, S.H. (1962). Temperature correction in conductivity measurements, *Limnol. Oceanogr.-Meth*., *7,* 330-334, doi:10.4319/lo.1962.7.3.0330

Stern, S.A., D.C. Slater, J. Scherrer, et al. (2008). ALICE: The Ultraviolet Imaging Spectrograph Aboard the New Horizons Pluto-Kuiper Belt Mission, *Space Sci. Rev. 140,* 155–187. doi:10.1007/s11214-008-9407-3

Thirouin, A., K.S. Noll, J.L. Ortiz, and N. Morales (2014). Rotational properties of the binary and non-binary populations in the trans-Neptunian belt. *Astron. Astrophys. 569*. doi:10.1051/0004-6361/201423567

Travis, B.J. and G. Schubert (2015). Keeping Enceladus warm, *Icarus 250,* 32-42. https://doi.org/10.1016/j.icarus.2014.11.017

Tsiganis, K., R. Gomes, A. Morbidelli, and H.F. Levison (2005). Origin of the orbital architecture of the giant planets of the Solar System. *Nature 435,* 459-461. https://doi.org/10.1038/nature03539

Tyler, G.L., I.R. Linscott, M.K. Bird, et al. (2008). The New Horizons Radio Science Experiment (REX), *Space Sci. Rev. 140,* 217–259. doi:10.1007/s11214-007-9302-3

Vernazza, P. et al. (2020). A basin-free spherical shape as an outcome of a giant impact on asteroid Hygiea. *Nat. Astron., 4*, 136–141. doi:10.1038/s41550-019-0915-8

Vokrouhlický, D., W.F. Bottke, and D. Nesvorný (2016). Capture of Trans-Neptunian Planetesimals in the Main Asteroid Belt. *Astron. J.* 152, 39. doi:10.3847/0004-6256/152/2/39

Walsh, K.J., A. Morbidelli, S.N. Raymond, D.P. O'Brien, and A.M. Mandell (2011). A low mass for Mars from Jupiter's early gas-driven migration. *Nature 475,* 206-209. doi:10.1038/nature10201

Weiss, B.P., V. Colicci, and J.B. Biersteker (2020). Searching for subsurface oceans on the moons of Uranus using magnetic induction. AGU Fall Meeting, Abstract GP33A-05.

Weiss, B.P., J.B. Biersteker, V. Colicci, A. Couch, A. Petropoulos and T. Balint (2021). Searching for subsurface oceans on the moons of Uranus using magnetic induction. Lunar and Planetary Science Conference 52, abstract #2096.

Zimmer, C., K.K. Khurana, and M.G. Kivelson (2000). Subsurface oceans on Europa and Callisto: Constraints from Galileo Magnetometer observations. *Icarus, 147,* 329-347. https://doi.org/10.1006/icar.2000.6456